# On the meridional extent and fronts of the Antarctic Circumpolar Current

ALEJANDRO H. ORSI,*† THOMAS WHITWORTH III,* and
WORTH D. NOWLIN Jr*

**Abstract**—Large-scale features of the Antarctic Circumpolar Current (ACC) are described using all historical hydrographic data available from the Southern Ocean. The geopotential anomaly of the sea surface relative to 1000 db reveals the highly-sheared eastward flow of the ACC and the strong steering of the current by the ridge system around Antarctica. The near-surface property distributions differentiate the ACC waters from the warmer and saltier waters of the subtropical regimes. The Subtropical Front (STF), interrupted only by South America, marks the northernmost extent of subantarctic waters. Distributions of properties on isopycnal surfaces show an abrupt end to the characteristic signal of the Upper Circumpolar Deep Water (UCDW), as this water mass shoals southward and is entrained into the surface mixed layer. This sharp water mass boundary nearly coincides with the southernmost circumpolar streamline passing through Drake Passage. To its south are the weakly-sheared circulations of the subpolar regime. Inspection of many hydrographic crossings of this transition reveals that the poleward edge of the UCDW signal is a reasonable definition of the southern boundary of the ACC. At Drake Passage, three deep-reaching fronts account for most of the ACC transport. Well-established indicators of the Subantarctic Front and Polar Front are traced unbroken around Antarctica. The third deep-reaching front observed to the south of the Polar Front at Drake Passage also continues with similar characteristics as a circumpolar feature. It is called here the southern ACC front. Stations from multiple synoptic transects of these circumpolar fronts are used to describe the average property structure within each ACC zone. Between the STF and the southern boundary of the ACC, the shear transport of the circumpolar current above 3000 m is at all longitudes about 100 Sv $(1 \text{ Sv} = 10^6 \text{ m}^3 \text{ s}^{-1})$ eastward.

## INTRODUCTION

Pronounced meridional gradients in surface properties separate waters of the Southern Ocean from the warmer and saltier waters of the subtropical circulations. Deacon (1933, 1937) called this hydrographic boundary the Subtropical Convergence, a term replaced by the Subtropical Front (STF) in recent years (Clifford, 1983; Hofmann, 1985). South of the STF is the eastward flow of the Antarctic Circumpolar Current (ACC), extending unbroken around the globe. It is driven by the world's mightiest westerly winds, found approximately between 45°–55°S (Trenberth *et al.*, 1990). Because of the land mass distribution (Fig. 1), the ACC is a unique global link that connects all major oceans. Specific water masses shoal dramatically southward across the Circumpolar Current, so

---

*Department of Oceanography, Texas A&M University, College Station, TX 77843, U.S.A.
†Presently at the Pacific Marine Environmental Laboratory, NOAA, Seattle, WA 98115, U.S.A.
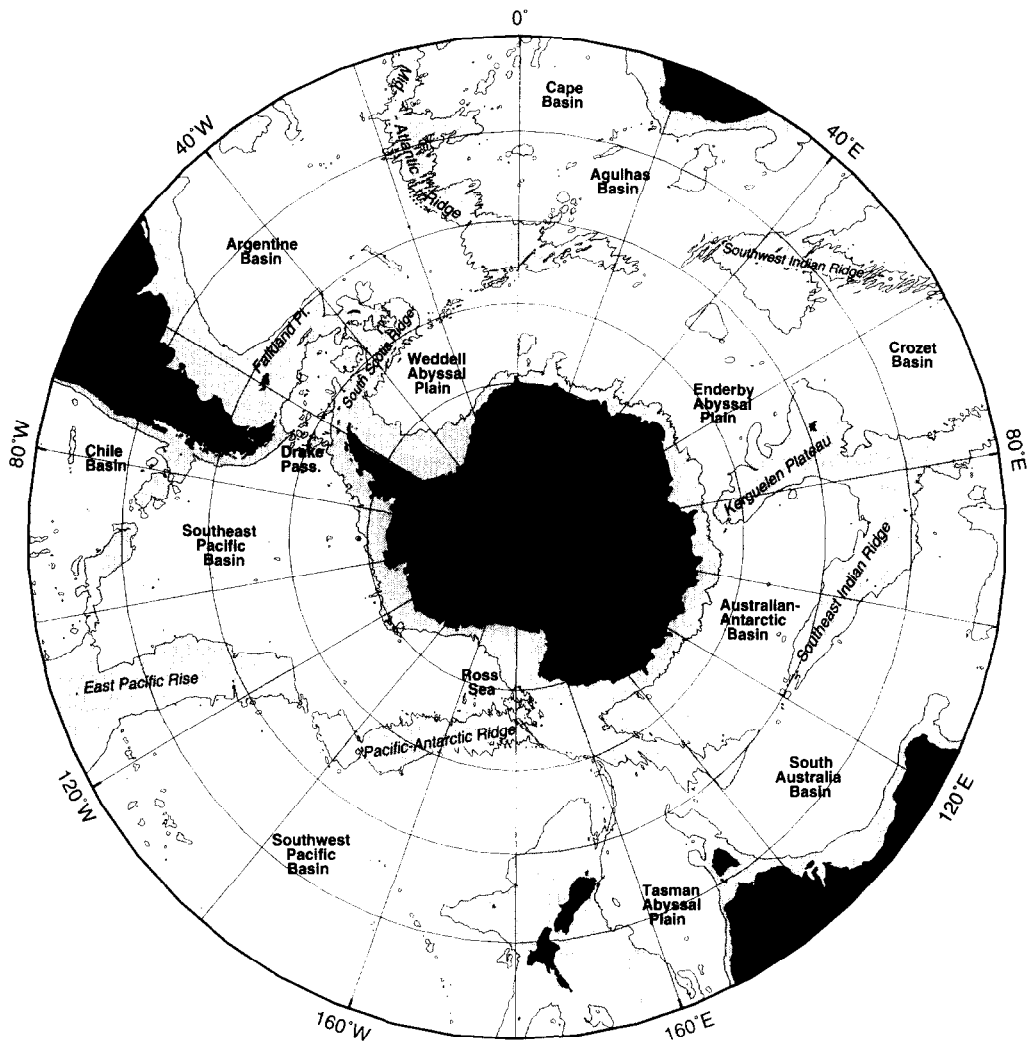
Fig. 1.    Principal bathymetric features of the Southern Ocean; depths less than 3500 m are shaded.

that deep waters originating farther to the north are able to enter the subpolar regime and mix laterally with Antarctic shelf waters.

In contrast to the long-established demarcation between the subtropical regime and the ACC, there is yet no well-defined boundary between this current and the subpolar regime. Deacon (1937) recognized a westward flow adjacent to Antarctica, which is driven by the prevailing easterly winds found to the south of about 65°S. Isotherms and isohalines shoal at the transition between west and east winds, inducing clockwise flow under geostrophic balance (Deacon, 1937, 1982).

Cyclonic cells of recirculating waters develop south of the ACC where it is located sufficiently far from the Antarctic Continent. The Weddell and Ross gyres are the best known of these subpolar cyclonic circulations (Deacon, 1933, 1979; Reid, 1965, 1986). A third smaller cell may also exist east of the Kerguelen Plateau (Deacon, 1937; Rodman and

Gordon, 1982; Tchernia and Jeannin, 1983). These clockwise circulations, together with the wind and buoyancy-driven westward flows over and near the continental slope (Gill, 1973; Gordon, 1988), form the subpolar regime of the Southern Ocean, i.e. the entire region to the south of the ACC.

The eastward flow of the ACC is associated with a steep rise of isopycnals toward the south through the entire water column. Deacon (1937) noted that the poleward rise of isotherms and isohalines was not uniform, but occurred in a series of clear step-like patterns. Bands of large horizontal density gradients characterize the ACC fronts, which are associated with strong surface currents (Nowlin et al., 1977). Extensive research and the availability of more closely-spaced data showed that two major fronts were continuous features of the ACC. Following Emery (1977) and Whitworth (1980), they are called the Subantarctic (SAF) and Polar (PF) Fronts. Peterson and Stramma (1991) give details on the evolution of these fronts' nomenclature.

At a few locations around the globe, closely-spaced stations reveal three frontal features within the ACC. In particular, a third deep-reaching front is observed persistently as part of the ACC to the south of the PF at Drake Passage (Nowlin et al., 1977; Roether et al., 1993). There, the distinct surface water mass regimes separated by the three ACC fronts have been called, from north to south (Whitworth, 1980): the Subantarctic Zone (SAZ), Polar Frontal Zone (PFZ), Antarctic Zone (AZ) and Continental Zone (CZ).

Gordon et al. (1977a) also found a frontal feature to the south of the PF in the western Scotia Sea; the Scotia Front is not part of the ACC, but separates waters of the ACC from those characteristic of the Weddell–Scotia Confluence (Gordon, 1967). At the Greenwich Meridian, Whitworth and Nowlin (1987) observed a similar front with associated shear at the boundary between the ACC and the Weddell Gyre. Smith (1989) interpreted this feature as the downstream expression of the Scotia Front; its continuity over the remainder of the circumpolar region is only a matter of speculation (Clifford, 1983). If this southern frontal feature is circumpolar, then a more general description and appropriate nomenclature are warranted.

The ACC is a critical component of the global ocean circulation; thus, it is important to clearly establish its spatial extent and describe its structure completely. Only then can one proceed with studies of the currents and property fluxes of the ACC separately from those of the adjacent subtropical and subpolar regimes.

This work is a new interpretation of the meridional extent and structure of the ACC based on analyses of historical station data available up to 1990 (Fig. 2). It provides an updated description to which newer, high-quality data gathered during the World Ocean Circulation Experiment can be compared. It also offers potential for new quantitative and theoretical studies of this current and its many interactions with the adjacent regimes.

To contrast the ACC with the adjacent subtropical and subpolar regimes, a brief review of the baroclinic flow of the Southern Ocean is presented in the next section, followed by verification that property distributions effectively mark the northern terminus of Subantarctic surface waters. Because the properties of surface waters give no clear indication of the southern extent of circumpolar circulation, a definition for the southern bound of the ACC is introduced, relying on the features observed within the underlying Circumpolar Deep Water (CDW). Closely-spaced stations along the Greenwich Meridian are used as a starting point in determining the characteristics of the ACC's poleward boundary.

With its meridional bounds clearly established, additional features of the ACC are classified more readily. A circumpolar deep-reaching front found south of the PF is
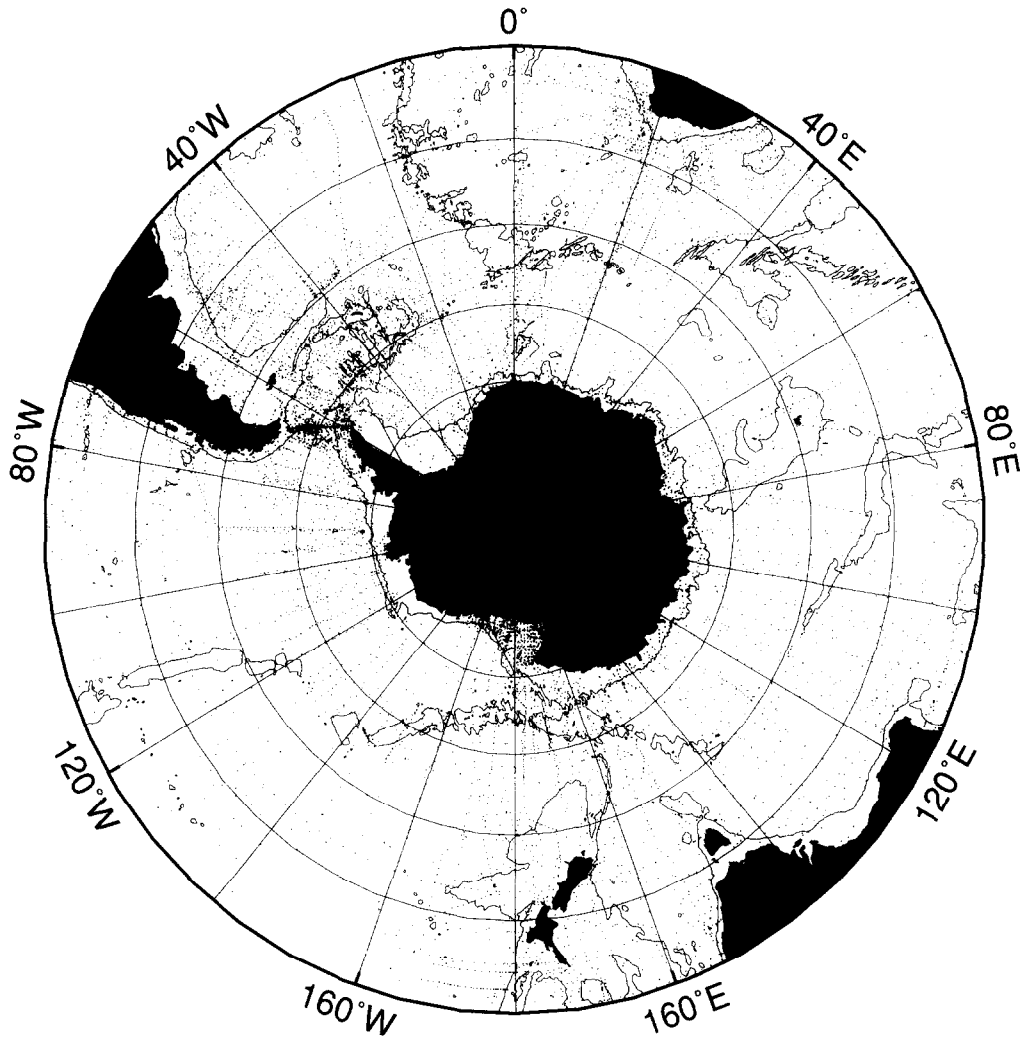
Fig. 2.  Positions of hydrographic stations used in this study; solid contour is the 3000 m isobath.

described. Also the baroclinic volume transport in the upper 3000 m of the ACC is estimated along its circumpolar extent.

## FLOW REGIME

Flow charts of the Southern Ocean are found in Gordon *et al.* (1978) and in the Southern Ocean Atlas (Gordon and Mollineli, 1982). However, over 2000 stations have been made south of 30°S since that atlas was completed. Fig. 3 shows the dynamic topography at 50 db relative to 1000 db. The 50 db horizon was selected to represent the near-surface geostrophic flow, while reducing possible seasonal variability in the data.

One way to visualize the ACC in Fig. 3 is to consider only the streamlines that pass through Drake Passage (Gordon *et al.*, 1978; Orsi *et al.*, 1993), the major constriction to
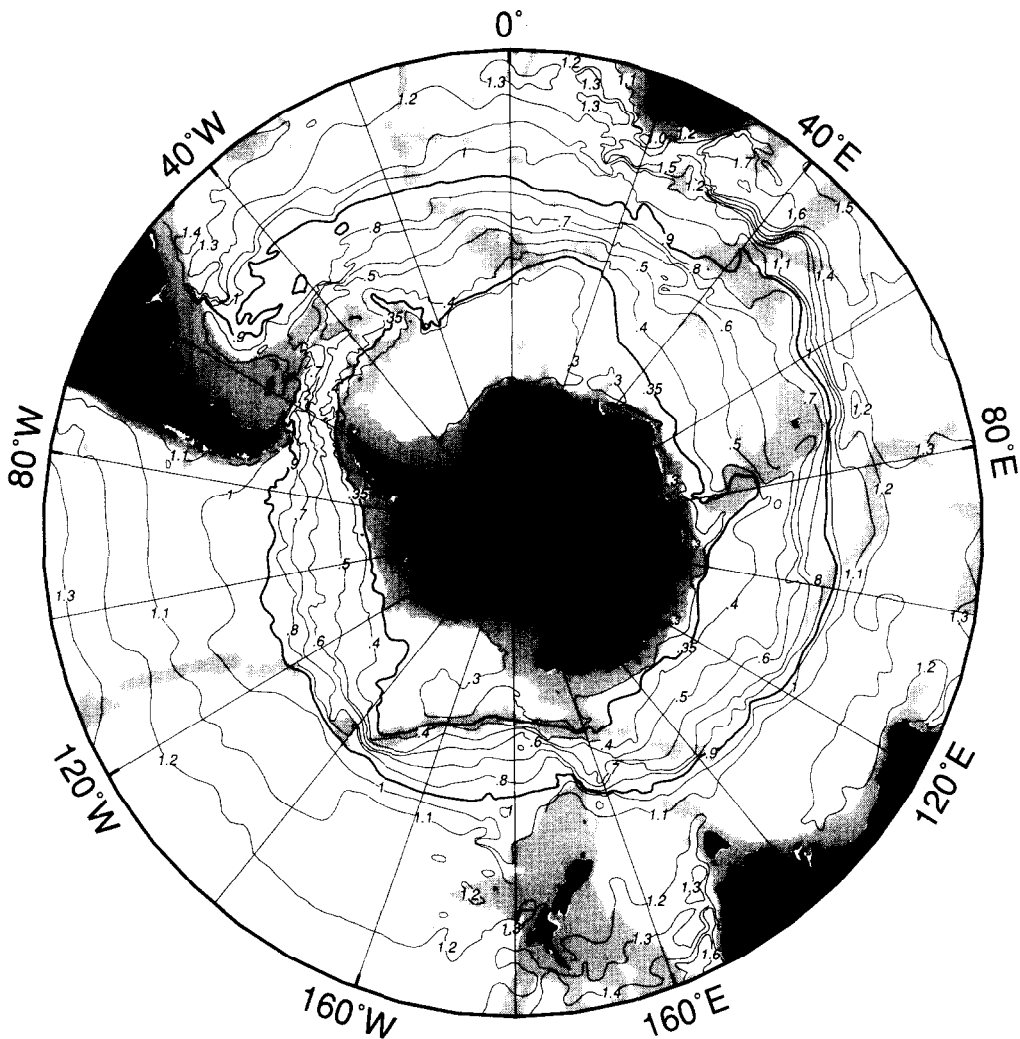
Fig. 3. Geopotential height anomaly at 50 db with respect to 1000 db, in dynamic meters
(10 J kg$^{-1}$); depths less than 3000 m are shaded.

circumpolar flow. On this basis, all contours with dynamic height values between 0.9 and
0.35 dyn m can be regarded as representing the ACC. The band of the ACC shows large
horizontal shear compared with the adjacent regions to the south and to the north,
particularly in the eastern sectors of the subtropical oceans. It is noted that parcels moving
along the edges of the ACC band can eventually exit the current as they interact more
readily with the adjacent circulations of the subtropical and subpolar regimes. But in a
mean sense, waters within the ACC band constitute a continuous circumpolar circulation.

As Gordon *et al.* (1978) noted, major bottom ridges firmly control the path of the ACC.
Sharp poleward shifts are observed in Fig. 3 through the broad gap in the Southwest Indian
Ridge, between 20° and 30°E (Deacon, 1979; Orsi *et al.*, 1993), and through the narrow

fractures zones in the Pacific–Antarctic Ridge, between 145° and 120°W (Patterson and Whitworth, 1990). Downstream of South America there is a sharp northward shift caused by the Scotia Arc. The ACC band seems to widen significantly in the southwestern Indian Ocean before it continues around the obstructing Kerguelen Plateau, which is oriented almost meridionally near 70°E.

Dynamic heights less than 0.35 dyn m represent the subpolar regime in Fig. 3. This regime shows small horizontal shear over the area of varying width adjacent to Antarctica. The weak cyclonic flow of the Weddell Gyre is suggested by the large area encompassed by the 0.3 dyn m streamline in the Atlantic sector. A smaller clockwise circulation extends northeast from the Balleny Islands, in the Ross Sea. East of the Kerguelen Plateau, where some investigators had suggested an even smaller subpolar gyral circulation, a sharp northward meander followed by southward return flow is indicated by the 0.35 and 0.3 dyn m isolines.

North of the ACC band, i.e. for dynamic heights larger than 0.9 dyn m, strong poleward flows are found near the western boundary of each ocean. These contours indicate the locations of the Brazil Current (1.0–1.4 dyn m), Agulhas Current (1.2–1.7 dyn m), and East Australian Current (1.2–1.6 dyn m). Their eastward extensions form the southern limbs of the subtropical gyres, where they are also known as the South Atlantic, South Indian Ocean, and South Pacific Currents (Stramma and Peterson, 1990; Stramma, 1992; Stramma *et al.*, 1995). These currents show considerable meridional shear over the western basins; at some locations, e.g. between 40° and 80°E, one sees no dynamical boundary between them and the circumpolar flow.

In contrast, the subtropical and circumpolar circulations seem quite distinct in the eastern sectors of the oceans. Moreover, over large areas, e.g. the southeastern Pacific, the waters found between the 0.9–1.2 dyn m contours in Fig. 3 are too cold and fresh to be part of the subtropical circulation. There the observed water mass structure is still characteristic of the Subantarctic regime. Thus, instead of the previous approximation in the dynamic topography, horizontal property maps are commonly used to define everywhere a more exact northern limit to subantarctic waters, and to separate them from the subtropical waters found farther to the north.

## NORTHERN EXTENT OF SUBANTARCTIC SURFACE WATER

The proximity of Subantarctic Surface Water (SASW) to the much warmer and saltier Subtropical Surface Water (STSW) produces large property gradients, the original indicators of the STF. Deacon (1937) gave the first global description of this upper-water front. He noted that regardless of the season or ocean basin, surface temperature (salinity) changes as large as 4–5°C (0.5) mark the location of the STF; its northern side is generally warmer (saltier) than 11.5°C (34.9) (Deacon, 1982).

Temperature and salinity distributions at 100 m were examined in lieu of Deacon's surface indicators of the STF. Its approximate location lies within a band (shaded in Fig. 4) across which temperatures increase northward from 10°C to 12°C, and salinities from 34.6 to 35.0 at 100 m. Since the salinity field shows smaller seasonality than temperatures, the haline gradient is the more reliable indicator (Deacon, 1982); one exception is the southeast Pacific sector.

The transition between SASW and STSW, as observed at 100 m (Fig. 4), is almost everywhere equatorward of the northernmost streamline representing the ACC (0.9 dyn
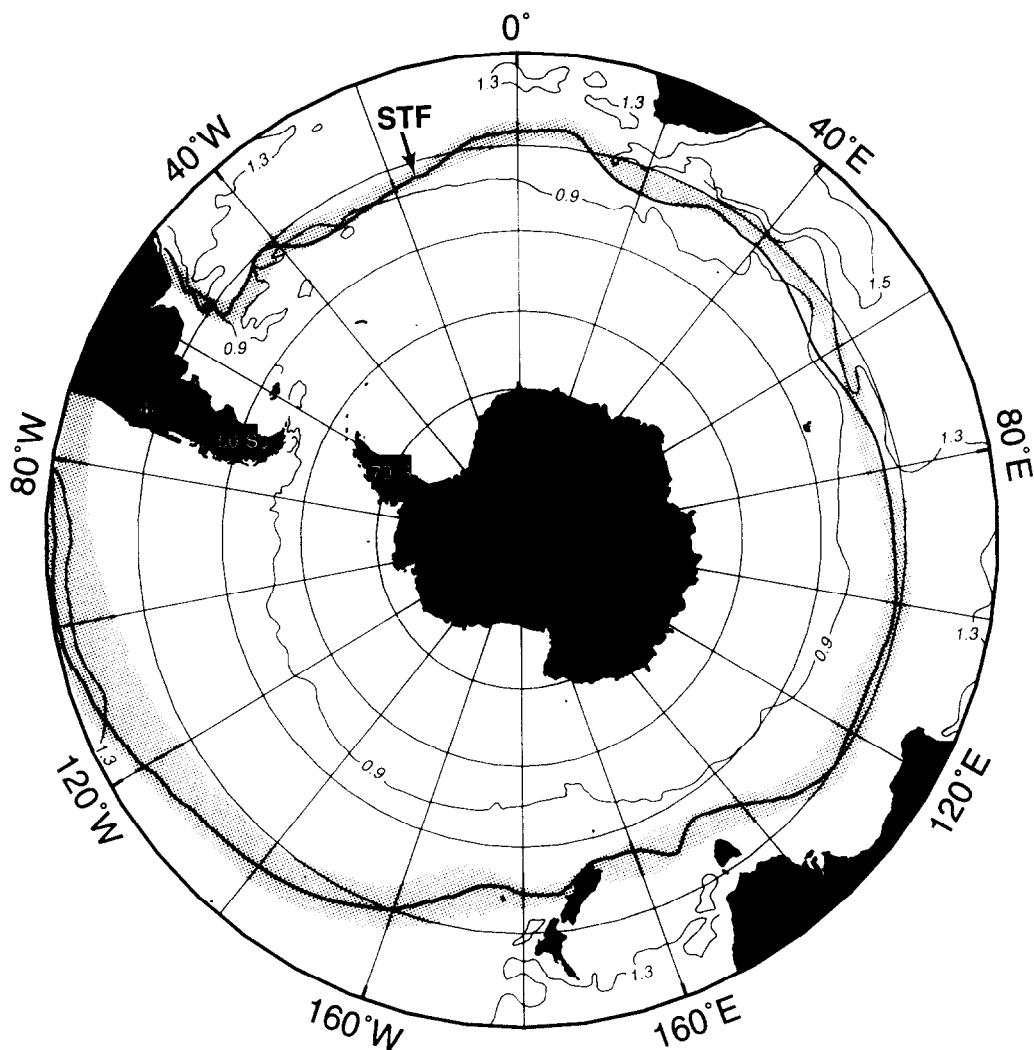
Fig. 4. Transition between SASW and STSW is indicated by the shaded band, within which temperatures (salinities) rise equatorward from 10°C to 12°C (34.6–35.0) at 100 m. Position of the STF (heavy solid line) from Deacon (1982); light lines are selected contours of geopotential height anomaly from Fig. 3.

m from Fig. 3). Also it is poleward of the closed circulations of the three subtropical gyres, e.g. to the south of the 1.3 (1.5) dyn m isolines in the Atlantic and Pacific (Indian) Oceans.

The transitional band is seen to widen in the southeast Pacific (east of 130°W). To its south there is a prominent low-salinity signal extending westward from Chile along 41°S (Deacon, 1937, 1977; Neshyba and Fonseca, 1980). The source of this signal is the high precipitation and river runoff (Pickard, 1971). Some of this relatively fresh SASW is also carried around the southern tip of South America, and over the eastern shelves of Argentina (Silva, 1977).

The latest global path of the STF, derived by Deacon (1982) from analyses of surface

properties, is indicated in Fig. 4 by the heavy line. In most regions it is within the transitional band of properties at the 100 m level. Minor differences are likely to result from inclusion of data collected after 1974, which were not considered by Deacon. Clearly the STF is not continuous through Drake Passage, and thus it cannot be considered part of the ACC. However, it is a reliable water mass boundary that separates the circumpolar regime from the subtropical regime to its north, marking everywhere the northern bound of SASW.

## POLEWARD EXTENT OF CIRCUMPOLAR CIRCULATION

Antarctic Surface Water (AASW) extends with rather uniform properties from the PF to the continental margins of Antarctica, where shelf waters are found at near freezing temperatures. Below AASW, the warm and saline water mass that occupies most of the deep layers of the ACC is the Circumpolar Deep Water (CDW). It is generally divided into Upper CDW (UCDW), characterized by low oxygen and high nutrient concentrations, and Lower CDW (LCDW), characterized by high salinities.

In contrast to the uniformity of AASW, the CDW shows significant alterations as it shoals toward the south. LCDW is dense enough to penetrate south of the ACC into the subpolar regime underneath the AASW, i.e. below direct surface influence. Its poleward spread often reaches the Antarctic continental shelves (Deacon, 1982). At several locations around Antarctica, LCDW mixes with shelf waters to form denser water that sinks downslope to its equilibrium level; this is often the ocean bottom (Foster and Carmack, 1976; Jacobs *et al.*, 1970). Dense Antarctic water spreads northward into the ACC, cooling and freshening the CDW. The resulting mixture eventually fills most of the World Ocean abyssal layers through a series of deep western boundary currents that branch off the ACC (Mantyla and Reid, 1983).

The previously described water mass changes are clearly indicated on property distributions from closely-spaced stations crossing completely the ACC and Weddell Gyre along the Greenwich Meridian (Whitworth and Nowlin, 1987). On the oxygen section shown in Fig. 5, the isopycnal $\sigma_0 = 27.6$ kg m$^{-3}$ lies very close to the $O_2$-min of the UCDW (Callahan, 1972; Reid, 1986). Also, this particular isopycnal is generally found within the characteristic nutrient maxima of UCDW (Sievers and Nowlin, 1984). The other two pictured isopycnals lie within the LCDW. Isopycnal $\sigma_0 = 27.79$ kg m$^{-3}$ follows the salinity and oxygen maxima of the North Atlantic Deep Water (NADW) that enters the ACC from the north in the southwestern Atlantic Ocean (Reid and Lynn, 1971; Reid *et al.*, 1977; Reid, 1989). The deepest isopycnal $\sigma_0 = 27.83$ kg m$^{-3}$ is within LCDW that participates in bottom water formation in the southwestern Weddell Sea (Orsi *et al.*, 1993).

From volume transport considerations Whitworth and Nowlin (1987) located the northern boundary of the Weddell Gyre at Sta. 80. They also described the frontal feature observed between Stas 79 and 80. This front is marked by increased isopycnal slopes (horizontal density gradient) in Fig. 5, and its presence is indicated by a prominent void in $\theta$-S space between those two stations (Whitworth and Nowlin, 1987). This station pair also spans the southernmost continuous streamline representing the ACC in Fig. 3 (0.35 dyn m).

At this particular location of the ACC there is a sharp boundary to the south of which no distinct UCDW signal is found. UCDW is supplied primarily from the eastern South Pacific Ocean and the western Indian Ocean (Callahan, 1972; Warren, 1981; Park *et al.*,

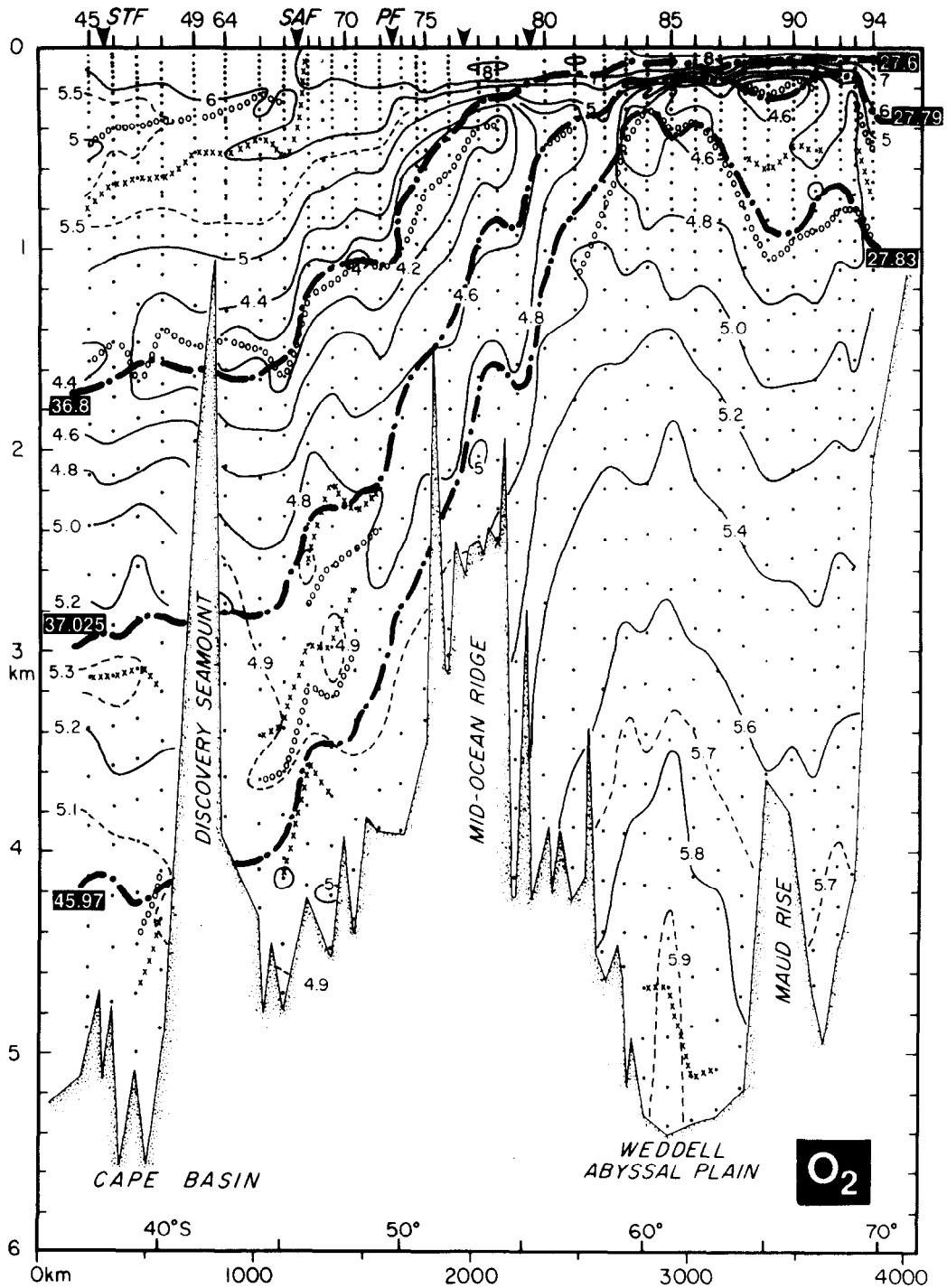Fig. 5.    Dissolved oxygen (ml l$^{-1}$) in vertical section at the Greenwich Meridian, from the AJAX expedition of January 1984. Heavy dash–dot lines from top to bottom are isopycnals $\sigma_0 = 27.6$ ($\sigma_2 = 36.8$) kg m$^{-3}$, $\sigma_0 = 27.79$ ($\sigma_2 = 37.025$) kg m$^{-3}$, and $\sigma_0 = 27.83$ ($\sigma_2 = 37.11$, $\sigma_4 = 45.97$) kg m$^{-3}$. Maxima (minima) are denoted by crosses (open circles).

1993); in Fig. 5 it is recognized clearly by $O_2 < 4.5$ ml $l^{-1}$ at density values of 27.35 kg m$^{-3}$ $< \sigma_0 < 27.75$ kg m$^{-3}$ (Sievers and Nowlin, 1984). Therefore, UCDW characteristics are found only to the north of Sta. 80. Although there are low-oxygen concentrations within the Weddell Gyre (Stas 80–94), they correspond to LCDW. There, both $O_2$-min cores seen in Fig. 5 lie near the S-max of the LCDW ($\sigma_0 = 27.79$ kg m$^{-3}$) and $\sigma_0 = 27.83$ kg m$^{-3}$, which corresponds approximately to the Central Intermediate Water (Whitworth and Nowlin, 1987; Orsi *et al.*, 1993).

Thus, the southward disappearance of the UCDW signal in Fig. 5 coincides with the boundary between the ACC and the Weddell Gyre. At this point the core of the UCDW has been entrained into the mixed layer of the subpolar regime; note that $\sigma_0 = 27.6$ kg m$^{-3}$ rises to less than 200 m at Sta. 80. To some extent, vertical mixing with the rising LCDW further diminishes the characteristic signal of the UCDW.

In their analysis of a meridional section near 135°W, Patterson and Whitworth (1990) similarly noted that no UCDW signal is found within the Ross Gyre. These observations raise the question of whether the southern terminus of UCDW characteristics could be used generally as a water-mass marker to identify the poleward extent of the circumpolar flow of the ACC.

## Southern limit of UCDW

Distributions of depth, potential temperature, salinity and oxygen concentration on isopycnal surfaces were prepared for the region south of 40°S, to establish the spatial extent of the UCDW core from its northern source regions. The oxygen distribution on $\sigma_0 = 27.6$ kg m$^{-3}$ is shown in Fig. 6. This isopycnal surface rises from about 1600 m near the STF to within 200 m of the sea surface over the region poleward of the 0.35 dyn m (dotted) contour in Fig. 3, i.e. south of the ACC band.

On this isopycnal, there is a broad zonal band in which oxygen varies only from about 4 ml $l^{-1}$ to 5 ml $l^{-1}$ (Fig. 6). As confirmed at the Greenwich Meridian, in the ACC (Stas 46–79 in Fig. 5) this isopycnal lies within the UCDW core, with little influence from the more ventilated waters above. The most striking feature in Fig. 6 is the narrow zonal band across which oxygen values increase from less than 5 ml $l^{-1}$ to greater than 7 ml $l^{-1}$. Similarly, temperatures (not shown) decrease from above 1°C to below −1°C and salinities decrease from about 34.5 to less than 34.4 across the same band. Waters observed to the south of this band are AASW and shelf waters, and show relatively small ranges of property values on isopycnal $\sigma_0 = 27.6$ kg m$^{-3}$. The band also includes the 0.35 dyn m contour, representing the southernmost circumpolar contour in Fig. 3.

In this study we use closely-spaced stations spanning this water mass transition to trace the southern extent of the UCDW signal. Property distributions were examined on 84 sections crossing that band (see Fig. 7 for section locations); their particulars are listed in Table 1. UCDW lies always below the fresher and colder AASW (S < 34.40, $\theta$ < 0.5°C), and above the much saltier LCDW (S > 34.70). Most of these sections show UCDW rising poleward to near 200 m with temperatures above 1.5°C and salinities above 34.5. The location of the southern edge of UCDW could usually be identified within a pair of consecutive stations. These sections are used to trace the water mass boundary around Antarctica along the path indicated by the heavy solid line in Fig. 7. Except near the Kerguelen Plateau, it is generally found very close to the 0.35 dyn m streamline from Fig. 3.
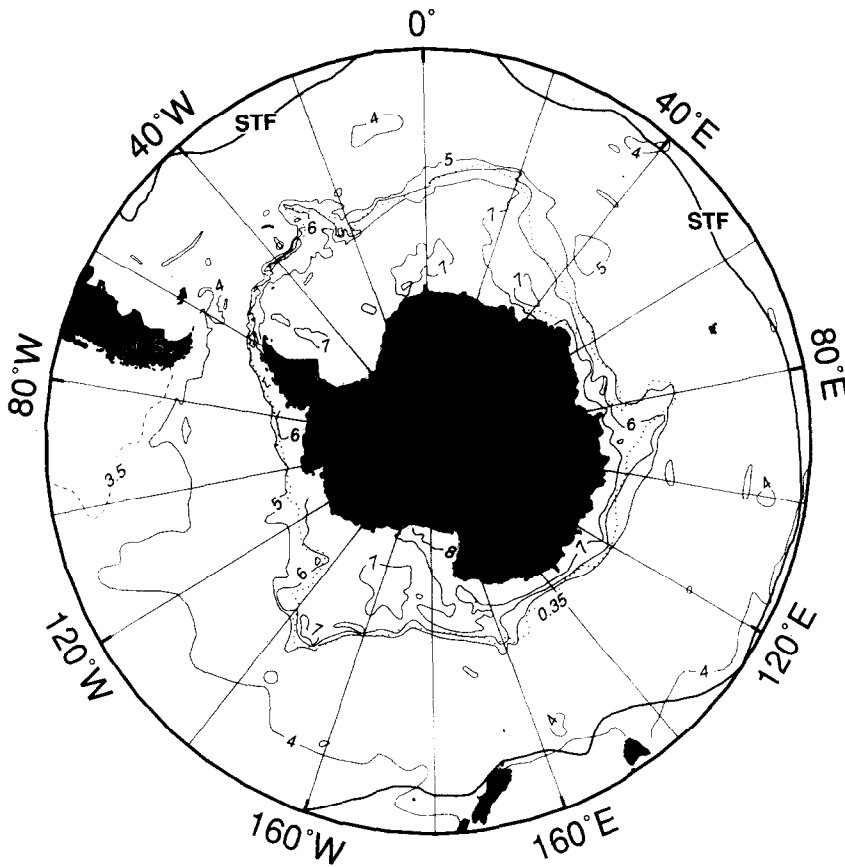
Fig. 6. Dissolved oxygen (ml l$^{-1}$) on the isopycnal defined by $\sigma_0 = 27.6$ ($\sigma_2 = 36.8$) kg m$^{-3}$ within the core of UCDW. The heavy line is the STF from Fig. 4; the dotted line is the 0.35 dyn m contour from Fig. 3.

The authors maintain that the southern terminus of UCDW characteristics constitutes a reasonable poleward boundary for the ACC: it marks the southern extent of the only water mass found exclusively in the ACC and not in the subpolar regime; and, farther south, the observed geostrophic shear is considerably weaker than within the ACC. Thus, it also marks the equatorward limit of the subpolar regime. The ACC boundary shown in Fig. 7 coincides with recent observations of the northern limits of the Weddell (Bagriantsev *et al.*, 1989; Smith, 1989; Orsi *et al.*, 1993) and Ross gyres (Reid, 1986; Patterson and Whitworth, 1990).

Regional details of the subpolar circulations are clearly indicated south of the southern ACC boundary shown in Fig. 7. Near 30°W, the boundary reflects the northward deflection of the northern limb of the Weddell Gyre around the South Sandwich Island Arc described by Orsi *et al.* (1993). Similarly, the northward turn seen between 145°E and 175°E agrees with the descriptions by Reid and Mantyla (1971) and Locarnini (1994), who speculate on the existence of a closed cyclonic cell to the north of the Balleny Islands (163°E) as part of the western Ross Gyre. Another small cell within the subpolar regime
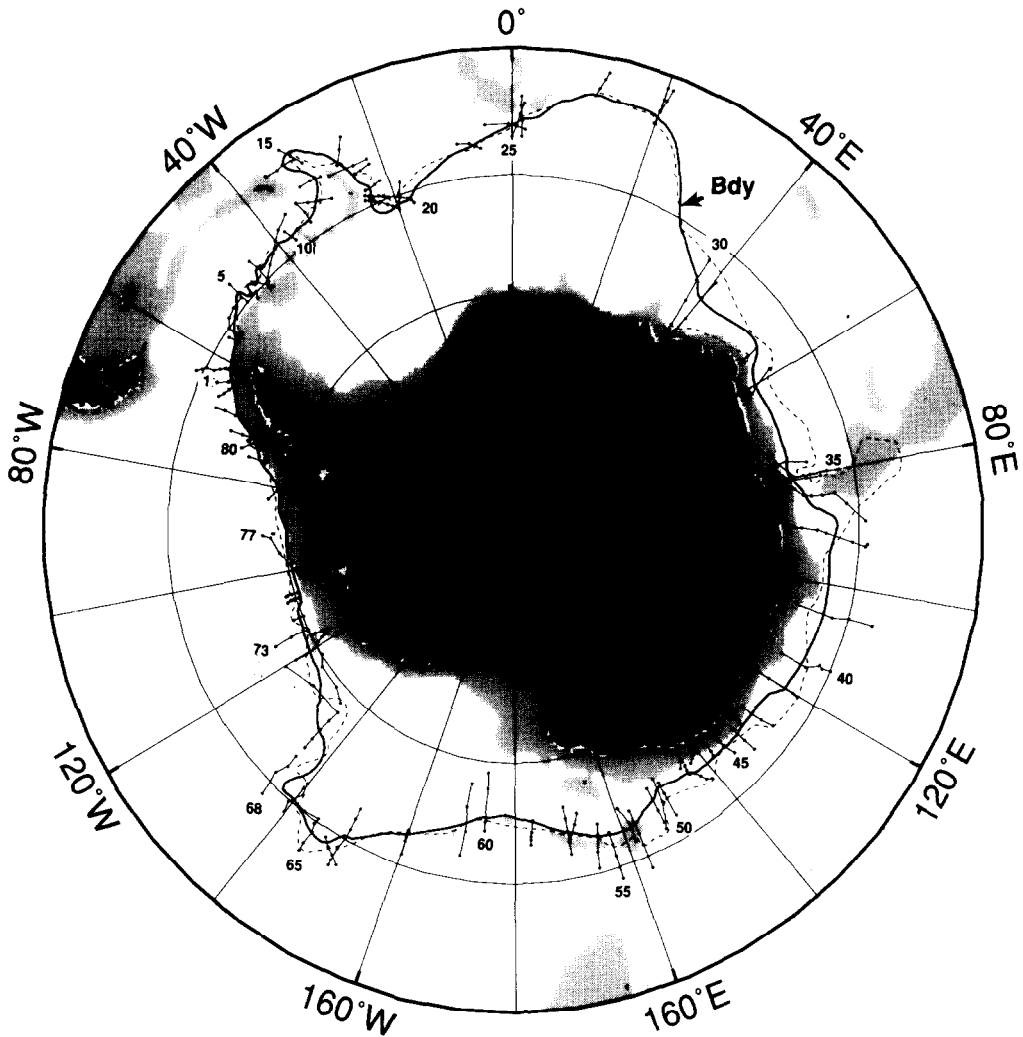
Fig. 7. Location of the southern boundary of the ACC (solid line) and of all synoptic sections listed in Table 1. Depths less than 2500 m are shaded; the dashed line is the 0.35 dyn m contour from Fig. 3.

may be located near 90°E, where the ACC boundary seems to depart southward from the 0.35 dyn m contour.

The close proximity of the ACC boundary to the Antarctic Continent over the regions between the Weddell and Ross gyres (Fig. 7) has important implications for processes leading to formation of Antarctic Bottom Water. Past the eastern ends of these subpolar cyclones, i.e. near 30°E and 130°W, the ACC flows southward and brings CDW close to the Antarctic Shelf Waters. Several sources of new deep and bottom waters have been reported east of the Weddell Gyre, e.g. near Prydz Bay (75°E; Jacobs and Georgi, 1977), Davis Sea (90–95°E; Treshnikov *et al.*, 1973), Shackleton Ice Shelf (95–105°E; Gordon, 1974), Adelie Coast (135–145°E; Gordon and Tchernia, 1972), and between 150°E and

160°E (Carmack and Killworth, 1978). East of the Ross Gyre, however, the ACC extends onto the continental slope, approximately between 100°W and 55°W (Z < 2500 m in Fig. 7); there the eastward flow of the ACC is forced northward by the Antarctic Peninsula. Limited observations available in the Bellingshausen Sea confirm the lack of Shelf Water (Potter and Paren, 1984; Talbot, 1988; Hofmann et al., 1993), one of the two required mixing components to form bottom water. Thus, production of water denser than CDW is unlikely in the southeastern Pacific Ocean.

*The ACC at Drake Passage*

Any new definition involving the ACC faces a stringent test at Drake Passage, the best-studied region of the ACC. We will show that the definition of the southern boundary is consistent, and that the boundary is distinct from the third front that has been observed here. The narrowness of Drake Passage has contributed some confusion in the nomenclature, which will be clarified.

Many closely-spaced stations were occupied at Drake Passage during the International Southern Ocean Studies (ISOS), 1974–1980. One of the first of these transects, section II from the R.V. *Melville* in 1975, extends from Cape Horn to the northern shelf of Livingston Island; Fig. 8 shows property distributions on its southern portion. Here the southern edge to UCDW characteristics is located over the continental slope (bottom depths near 1500 m). It was crossed twice within a two-day period: southward on 27 February (Stas 5–6), and again northward on 28 February (Stas 7–8).

Large southward decreases in temperature and salinity within the UCDW were observed on this section; but that water extends to Sta. 5, where at depths near 400 m oxygen was less than 4.4 ml $l^{-1}$, temperature above 1.6°C and salinity greater than 34.6 Sievers and Nowlin (1988) noted that UCDW extends southward over the continental slope in Drake Passage. In contrast, surface waters ($O_2 > 5$ ml $l^{-1}$, $\theta < 1$°C, and S < 34.4) very similar to those observed at the upper levels of the northern Bransfield Strait (Sievers and Nowlin, 1988) entirely occupy the density space $\sigma_0 < 27.75$ kg m$^{-3}$ at Stas 6 and 7.

The water mass boundary observed between Stas 5 and 7 (Fig. 8) clearly separates the ACC from the subpolar regime. Relative to the bottom, all waters north of Sta. 7 flow eastward as part of the ACC, as inferred from the general rising of isopycnals toward the south. Farther to the south, the flow over the continental slope is to the west as reported by Whitworth et al. (1982) who combined direct current measurements with hydrographic sections made from the *Melville* and *Yelcho* in 1979 and from the *Atlantis II* in 1980. In addition, year-long current measurements at two slope moorings revealed a persistent westward current within the subpolar regime, presumably as part of the Antarctic Polar Slope Current (Nowlin and Zenk, 1988).

Nowlin et al. (1977) located the southernmost deep-reaching front of the ACC between Stas 8 and 9 just north of its poleward boundary in Fig. 8. A repeat of this section (*Melville* Section V), carried out only three weeks later, crossed this front at the same location (Stas 53–55). Nowlin et al. (1977) did not assign any name to the deep-reaching front observed south of the PF. However, the term Continental Water Boundary (Whitworth, 1980; Sievers and Nowlin, 1984) is often used in the literature starting with Sievers and Emery (1978). They coined that name to define the northern limit of cold subsurface waters ($\theta < 0$°C between 150–500 m) that originates in the northern Bransfield Strait, which they called continental slope water.

*Table 1. Selected sections across the southern boundary of the ACC*

| | Ship | Cruise | Month-Year | Stations |
|---|---|---|---|---|
| 1 | *Melville* | III | Mar. 1975 | 35, 36, 37, 57 |
| 2 | *Melville* | II | Feb. 1975 | 14, 13, 12, 4, 53, 9, 8, 5, 7, 6 |
| 3 | *Conrad* | 18 | Feb. 1975 | 339, 341 |
| 4 | *Knorr* | AJAX | Jan. 1984 | 134, 133, 132, 131, 130 |
| 5 | *Conrad* | 18 | Feb. 1975 | 349, 348, 347 |
| 6 | *Knorr* | AJAX | Jan. 1984 | 129, 125, 126 |
| 7 | *Meteor* | 11/5 | Feb. 1990 | 122, 123 |
| 8 | *Eltanin* | 7 | Feb. 1963 | 98, 99, 100 |
| 9 | *Knorr* | AJAX | Jan. 1984 | 117, 118, 119, 120, 121, 122 |
| 10 | *Eltanin* | 9 | Aug. 1963 | 180, 181, 182 |
| 11 | *Eltanin* | 9 | Sep. 1963 | 186, 185, 184 |
| 12 | *Knorr* | AJAX | Jan. 1984 | 116, 115, 114, 113 |
| 13 | *Discovery* | | Feb. 1930 | 360, 361, 362 |
| 14 | *Discovery* | | 1930,1932 | 312, 502, 794, 1050 |
| 15 | *I. Orcadas* | 11 | Nov. 1976 | 9, 10, 11 |
| 16 | *I. Orcadas* | 16 | Apr. 1978 | 204, 203, 202 |
| 17 | *I. Orcadas* | 11 | Nov. 1976 | 15, 16, 17 |
| 18 | *I. Orcadas* | 7–75 | Dec. 1975 | 513, 514, 515 |
| 19 | *Meteor* | 11/5 | Feb. 1990 | 134, 135, 136, 137 |
| 20 | *Knorr* | AJAX | Jan. 1984 | 108–99 |
| 21 | *I. Orcadas* | 16 | May 1978 | 238, 237, 236, 235, 234, 233, 232 |
| 22 | *I. Orcadas* | 16 | May 1978 | 230, 231, 232 |
| 23 | *Meteor* | 11/5 | Feb. 1990 | 145, 146, 147 |
| 24 | *I. Orcadas* | 11 | Nov. 1976 | 24,26,27 |
| 25 | *Meteor* | 11/5 | Feb. 1990 | 154, 153, 152, 151 |
| 26 | *Knorr* | AJAX | Jan. 1984 | 76, 77, 78, 79, 80, 81 |
| 27 | *I. Orcadas* | 11 | Dec. 1976 | 38, 37, 35, 34 |
| 28 | *Vieze* | 716 | Feb. 1980 | 29, 30, 31, 32 |
| 29 | *I. Orcadas* | 12 | Jan. 1977 | 69, 70, 71, 72 |
| 30 | *Conrad* | 17 | Mar. 1974 | 277, 275, 274, 273, 271 |
| 31 | *Ob* | | Feb. 1957 | 217, 219, 221, 222 |
| 32 | *Discovery* | | Jan. 1930 | 45, 44, 43 |
| 33 | *Conrad* | 17 | Jan. 1974 | 244, 242, 240, 239, 238 |
| 34 | *Ob* | | Jan. 1957, **Mar. 1961** | 180, **618**, 183, 184 |
| 35 | *Dufresne* | 8405 | Jan. 1985 | 6, 7, 10, 12, 13 |
| 36 | *Eltanin* | 47 | Feb. 1947 | 1281, 1290, 1285, 1286 |
| 37 | *Eltanin*, **Ob** | 47, **6** | *Mar.* 1971 **Dec. 1960** | 1296, 1295, 1294, 1293, 1291 **543, 551** |
| 38 | *Melville* **Discovery**, *Eltanin* | | Feb. 1978 **Feb. 1951**, **Dec. 1970** | 432, **2810, 2811,** *2411*, **2812**, 100 |
| 39 | *Eltanin* | 50, **46** | Nov. 1971, **Dec. 1970** | 1406, 1407, 1412, **2409** |
| 40 | *Eltanin* | 45, **46** | Oct. 1970, **Dec. 1970** | 1255, 1253, 1254, 2407, **2408** |
| 41 | *Eltanin* | 44, **50** | Aug. 1970, **Nov. 1971** | 1233, **1431, 1432** |

*Table* 1.   *Continued*

| | Ship | Cruise | Month-Year | Stations |
|---|---|---|---|---|
| 42 | *Eltanin* | 37 | Feb. 1969 | 1090, 1088, 1086, 1085 |
| 43 | *Eltanin* | 37 | Feb. 1969 | 1079, 1081, 1083 |
| 44 | *Eltanin* | 41 | Jan. 1970 | 2311, 2308, 2310, 2309 |
| 45 | *Eltanin* | 50, **37** | Dec. 1971, **Feb. 1969** | 1447, **1069, 1070** |
| 46 | *Eltanin* | 37 | Feb. 1969 | 1067, 1065, 1063, 1062 |
| 47 | *Eltanin* | 37 | Jan. 1969 | 1005, 1007, 1009, 1011 |
| 48 | *Eltanin* | 50 | Dec. 1971 | 1460–1468, 1474, 1472 |
| 49 | *Eltanin* | 37 | Jan. 1969 | 993, 994, 996, 998 |
| 50 | *Volna* | 1348 | Feb. 1981 | 35, 36, 37, 38 |
| 51 | *Washington* | ARII | Jan. 1971 | 21, 20, 19, 18 |
| 52 | *Vieze* | 1347 | Feb. 1981 | 23, 22, 21, 20 |
| 53 | *Volna* | 1348 | Jan. 1981 | 9, 10, 11, 12, 13, 14 |
| 54 | *Washington* | ARII | Jan. 1971 | 3, 4, 6 |
| 55 | *Volna* | 1348 | Jan. 1981 | 2, 3, 4, 5, 6 |
| 56 | *Washington* | ARII | Jan. 1971 | 25, 26, 27, 28 |
| 57 | *Washington* | ARII | Jan. 1961 | 37, 36, 35 |
| 58 | *Eltanin* | 50 | Dec. 1971 | 1518, 1516, 1514, 1512, 1508 |
| 59 | *Eltanin* | 32 | Feb. 1968 | 793, 791, 789, 787, 786 |
| 60 | *Knorr*, *Melville* | KN73, GEO | Oct. 1978, Feb. 1974 | 77, 78, 79, **288, 287** |
| 61 | *Hakuho M.* | KH68 | Jan. 1969 | 45, 46, 47, 48 |
| 62 | *Eltanin* | 14 | Aug. 1964 | 340, 341, 342, 344, 343 |
| 63 | *Ferncroft* | | Jan. 1948 | 29, 28, 27, 26, 25, 24, 23 |
| 64 | *Staten I.* | | Jan. 1961 | 34, 35, 36, 37 |
| 65 | *Eltanin* | 20 | Oct. 1965 | 474, 475, 476, 477, 478 |
| 66 | *Eltanin* | 19 | Aug. 1965 | 459, 460, 461, 462 |
| 67 | *Eltanin* | 20 | Oct. 1965 | 478, 479, 480 |
| 68 | *Eltanin* | 17 | Mar. 1965 | 408, 409, 410, 411 |
| 69 | *Eltanin* | 17 | Apr. 1965 | 412, 413, 414, 415, 416 |
| 70 | *Eltanin* | 33 | Apr. 1968 | 814, 815, 816, 817, 818 |
| 71 | *Eltanin* | 17 | Apr. 1965 | 416, 417, 418 |
| 72 | *Eltanin*, **Staten I.** | 33 | Apr. 1968, Jan. 1961 | 820, 919, 818, **39, 40, 41, 42** |
| 73 | *Eltanin*, **Staten I.** | 11 | Jan. 1964, **Jan. 1961** | **243**,244,245,**46,45,44,43,42** |
| 74 | *Staten I.* | | Jan. 1961 | 51, 50, 49 |
| 75 | *Staten I.* | | Feb. 1961 | 54, 60, 59, 58 |
| 76 | *Staten I.* | | Feb. 1961 | 55, 61, 56, 57 |
| 77 | *Eltanin*, **Staten I.** | 11 | Jan. 1964, **Mar. 1961** | 252, 251, 250, 249, **79, 78** |
| 78 | *Eltanin* | 42 | Mar. 1970 | 1175, 1176, 1177, 1178, 1179 |
| 79 | *Eltanin* | 5 | Oct. 1962 | 42, 40, 41 |
| 80 | *Discovery* | | Jan. 1931 | 590, 589, 588, 587, 586, 585 |
| 81 | *Eltanin* | 5 | Oct. 1962 | 45, 44, 43 |
| 82 | *Ferncroft* | | Feb. 1948 | 56, 59, 58, 57 |
| 83 | *Eltanin* | 5 | Oct. 1962 | 35, 36, 37, 38, 39 |
| 84 | *Meteor* | 11/5 | Feb. 1990 | 114, 115, 116, 117 |
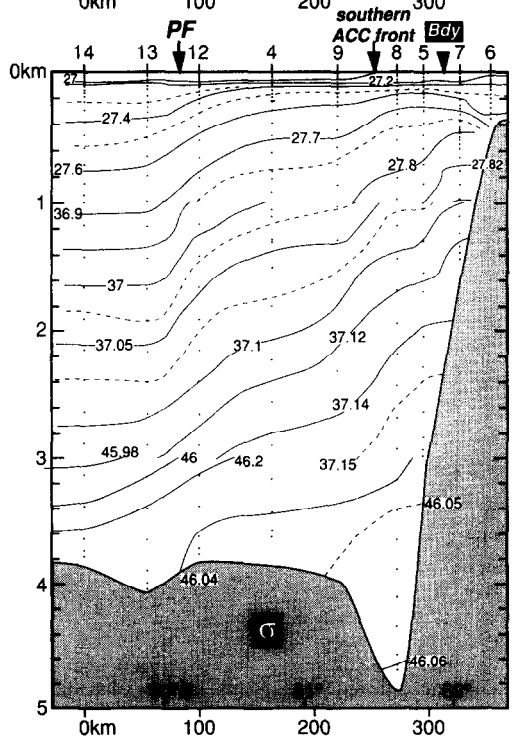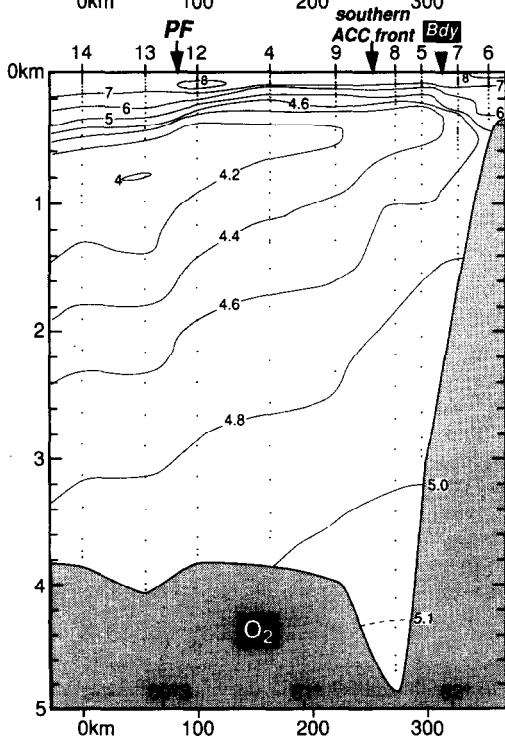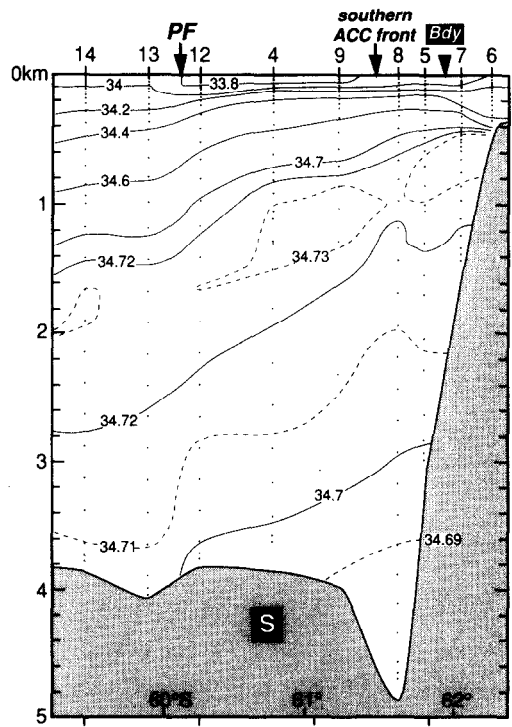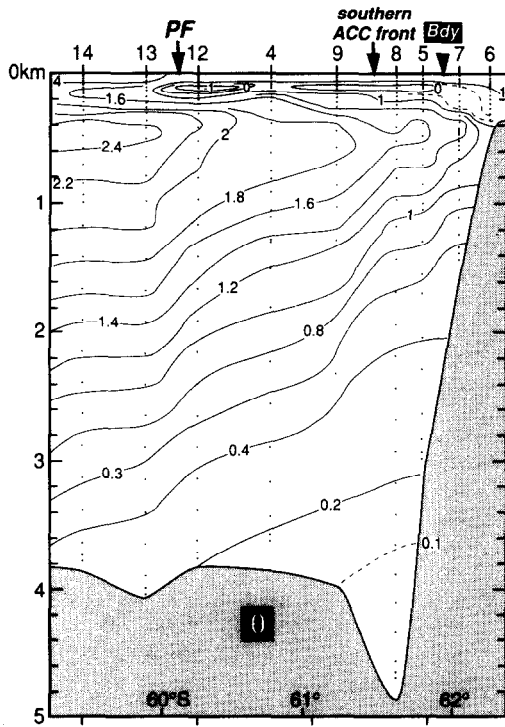
Thus, the term Continental Water Boundary was used to delineate the northern boundary of waters found to the south of the ACC, and not as a name for the deep-reaching frontal feature to the north of this boundary. In eight of the 12 XBT sections shown by Sievers and Emery (1978) this water mass boundary was identified by large horizontal temperature gradients at intermediate depths. Although similar thermal changes are seen south of 63°S on four other sections, e.g. their Hero sections 4–6 near 63°W, they did not label them as a water boundary. In any case, the term Continental Water Boundary, whether in reference to the southernmost deep-reaching front in the ACC or to the southern boundary of the ACC, is meaningful only in a very limited region near Drake Passage. Since the southern boundary of the ACC (and hence any additional ACC front south of the PF) is usually quite far north of the Antarctic Continent, the authors propose that this misleading term be abandoned.

Although the southernmost front of the ACC and the poleward edge of the UCDW signal often may be located adjacent to one another in Drake Passage, they are distinct features (Fig. 8). The first is a deep-reaching current core, a part of the Circumpolar Current, while the second feature is a water mass boundary that represents the southern boundary of the ACC. Because of their proximity, a single pair of stations spans both features in some sections across the southern Drake Passage, especially for stations more than 50 km apart. Coarser sampling probably prevented previous differentiation of these features, and may have influenced the assignment of the name Continental Water Boundary both to the current core and to the water mass boundary.

## CIRCUMPOLAR FRONTAL STRUCTURE

The two previous sections describe the observed water mass properties that define the northern extent of SASW and the southern extent of UCDW. These limits encompass a circumpolar band with large geostrophic shear (the ACC) compared to those to the north and south. The current cores within the ACC are examined in this section.

Many regional studies (Emery, 1977; Gordon et al., 1977b; Heath, 1981) indicated that within some longitude bands the ACC contains two current cores: the SAF and PF. Examining historical data, Clifford (1983) showed this to be the case along the entire path of the ACC, as Hofmann (1985) verified using drifter trajectories around Antarctica. Comparison of these previous studies with the position of the southern boundary of the ACC given in Fig. 7, reveals a wide band of ACC waters south of the PF. Starting with the best sampled locations, that band is examined for additional fronts or other features that might be circumpolar in extent.

### Southern ACC Front

Three deep fronts are seen within the ACC on many crossings of Drake Passage (Table 2). These fronts are clearly indicated in synoptic vertical sections by their large horizontal property gradients (Nowlin and Clifford, 1982) and pronounced isopycnal tilt throughout

Fig. 8. ($\theta$) Potential temperature (°C), (S) salinity, ($O_2$) dissolved oxygen (ml l$^{-1}$), and ($\sigma$) potential density anomaly $\sigma_0$, $\sigma_2$ and $\sigma_4$ (kg m$^{-3}$) in vertical section at Drake Passage, from the R.V. *Melville* section II of 1975 (section number 2 in Table 1). The southern limit of UCDW is labeled Bdy.

*Table* 2.    *Synoptic sections selected at Drake Passage, with location of the three ACC fronts denoted by asterix between stations—from left to right: SAF, PF, and southern ACC front; total geostrophic transport* ($T_t$) *relative to 3000 m, or deepest common depth* (Sv)

| | Section, with stations and ACC fronts position | $T_t$ |
|---|---|---|
| 1 | *Melville* 1975, Section II | |
| | 27, 26, 24, 23 * 20, 18, 16 * 15, 14, 13, 12, 4, 53, 9 * 8, 5, 7, 6 | 104 |
| 2 | *Melville* 1975, Section III | |
| | 29, 30 * 31, 32 * 33, 34, 35 * 36, 37, 57 | 110 |
| 3 | *Melville* 1975, Section IV | |
| | 46, 45, 44 * 43 * 42, 41, 40 * 39, 38 | 80 |
| 4 | *Melville* 1975, Section VI | |
| | 90, 89, 88, 87 * 80 * 65 * 64, 63, 61 | 77 |
| 5 | *Islas Orcadas* 1975 | |
| | 2, 3 * 6, 9, 12, 15 * 18, 21, 23, 25 * 27, 29 | 99 |
| 6 | *Conrad* 1975, Cruise 18 | |
| | 333, 334 * 335 * 336, 337 * 338, 339, 341, 342 | 92 |
| 7 | *Thompson* 1976, Section I | |
| | 1, 2, 3, 4 * 5, 9, 10, 11 * 12, 13, 16, 17, 18, 19, 21 * 20, 22 | 97 |
| 8 | *Thompson* 1976, Section II | |
| | 26, 27, 28, 29 * 30, 32, 34, 36, 38 * 40, 42, 43, 44, 45, 46, 47 * 48, 49 | 111 |
| 9 | *Melville* 1977 | |
| | 1, 2 * 3, 4, 37, 36 * 35, 34, 33, 5, 6 * 7, 8 | 75 |
| 10 | *Melville* 1979 | |
| | 11, 12, 13 * 14, 15, 16, 17, 10 * 9, 8, 7, 6, 5, 4 * 3, 2, 1 | 111 |
| 11 | *Yelcho* 1979 | |
| | 1, 2, 3, 4, 5, 6 * 7, 8, 9, 10 * 11, 12, 13, 14 * 15, 16, 17, 19 | 96 |
| 12 | *Atlantis* 1980, Cruise II | |
| | 23, 24, 25, 26, 27, 28 * 29, 30, 31 * 32, 33, 34, 35, 36 * 37, 38, 39 | 106 |
| 13 | *Meteor* 1990, Cruise 11/5 | |
| | 103, 104 * 105, 106, 107, 108, 109, 110, 111 * 112, 113, 114, 115 * 116, 117 | 107 |

the deep water column. UCDW is present at the southern front of the ACC with $\theta > 1.8°C$ in all thirteen transects listed in Table 2. This front is always found in waters deeper than 3500 m. After a northward turn around the Shackleton Fracture Zone, it continues eastward into the Scotia Sea.

Farther east, one location where the entire ACC has been sampled in good detail is the Greenwich Meridian. There, three deep-reaching fronts are observed between the STF and the southern boundary of the ACC (Fig. 9). They are evident in the density field shown in Fig. 9 as bands of enhanced isopycnal tilt; the third front is located south of the PF between Stas 76–77. There the UCDW has temperatures greater than 1.8°C (see Fig. 2 of Whitworth and Nowlin, 1987), i.e. the same characteristic found at Drake Passage at the southernmost front in the ACC. Hereafter this front is referred to as the southern ACC front. It is the only ACC front that does not separate distinct surface water masses: recall that the surface between the PF and the Antarctic Continental Shelf consists of AASW.

Summarized in Fig. 10 are some general features in the temperature and salinity fields that mark the position of the three ACC fronts at the Greenwich Meridian. Following Whitworth and Nowlin (1987) the SAF position is indicated by the rapid northward sinking of the salinity minimum associated with the Antarctic Intermediate Water (AAIW), from near the surface in the PFZ (S < 34) to depths greater than 400 m in the SAZ (S < 34.30).
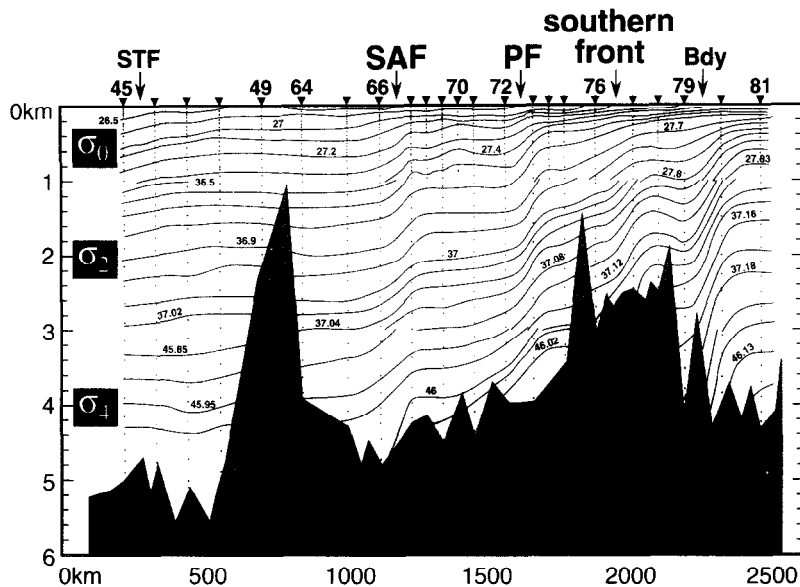
Fig. 9.   Potential density anomaly $\sigma_0$, $\sigma_2$ and $\sigma_4$ (kg m$^{-3}$) in vertical section along the Greenwich
Meridian, from the AJAX expedition of January 1984.

The large temperature gradient along the temperature minimum of the AASW, which starts to descend northward (Gordon, 1967), indicates the position of the PF. At the position of the southern ACC front there is a distinct temperature gradient along the $\theta$-max of the UCDW, as it shoals southward to near 500 m ($\theta > 1.8°C$). Note that all three ACC fronts appear as maxima in geostrophic volume transport relative to a deep common level (Fig. 10). Also at this longitude the station pair spanning the southern boundary of the ACC (79–80) carries a significant volume of water, although less than the southern front of the ACC (76–77) when referred to 1000 m.

Large isopycnal tilt is the principal indicator of the ACC fronts. However, often the station spacing is not as close as those at Drake Passage and the Greenwich Meridian. To unambiguously differentiate between the fronts on a given section, the information obtained from the density field was supplemented by examining various indicators of

Table 3.   Property indicators of the three ACC fronts

| SAF: | $S < 34.20$ at $Z < 300$ m, farther south |
| | $\theta > 4$–$5°C$ at 400 m, farther north |
| | $O_2 > 7$ ml l$^{-1}$ at $Z < 200$ m, farther south |
| PF: | $\theta < 2°C$ along the $\theta$-min at $Z < 200$ m, farther south |
| | $\theta$-min (if present) at $Z > 200$ m, farther north |
| | $\theta > 2.2°C$ along the $\theta$-max at $Z > 800$ m, farther north |
| southern: | $\theta > 1.8°C$ along $\theta$-max at $Z > 500$ m, farther north |
| | $\theta < 0°C$ along $\theta$-min at $Z < 150$ m, farther south |
| | $S > 34.73$ along S-max at $Z > 800$ m, farther north |
| | $O_2 < 4.2$ ml l$^{-1}$ along $O_2$-min at $Z > 500$ m, farther north |
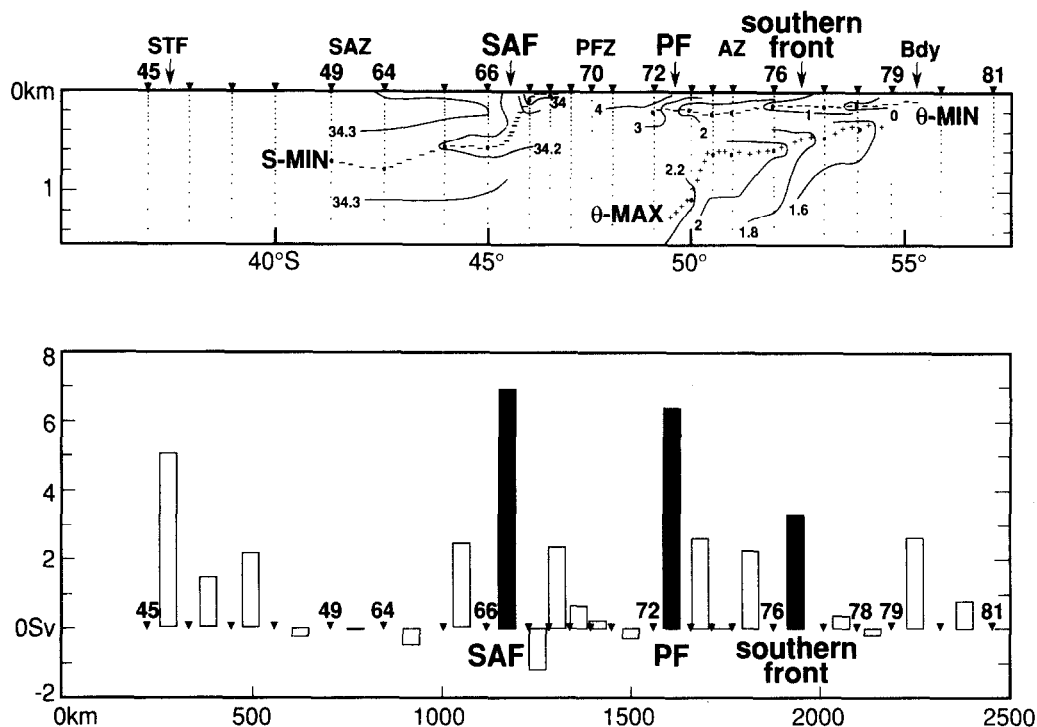
Fig. 10. Phenomenological indicators for the three ACC fronts in vertical section at the Greenwich Meridian: top, selected isohalines (isotherms) along the S-min ($\theta$-min and $\theta$-max); bottom, geostrophic volume transport (Sv) above and relative to 1000 m.

change in property distributions at each front. Table 3 lists several property indicators based on observations made at many locations around the globe (Gordon, 1967, 1971; Nowlin and Clifford, 1982; Whitworth and Nowlin, 1987). Due to the regional variability observed on these property fields (Gordon and Mollineli, 1982), one or more of these frontal indicators may not apply at some particular location of the ACC.

The triple frontal structure for the ACC was confirmed on all thirty-two of the available synoptic sections shown in Fig. 11; their particulars are listed in Table 4. Using the property indicators discussed before, the three ACC fronts were located between consecutive stations on each section in Fig. 11. Volume transports relative to 3000 m were also computed for all these sections; a subset is shown as bar-plots in Fig. 12 for approximately evenly-spaced locations around the globe. Again, in spite of sampling bias, relative volume transports for the station pairs spanning the three ACC fronts generally are larger than for adjacent station pairs.

To obtain more details about the frontal paths in the connecting areas between the sections listed in Tables 2 and 4, all available crossings of either one or two of the ACC fronts also were considered. Transport and property indicators of each ACC front were examined for numerous additional transects (95, 81 and 71 for the SAF, PF and southern ACC front, respectively).

Figure 11 shows the circumpolar paths of the three ACC fronts based on this examination. The SAF and PF are quite close to one other in many areas. Moreover, they may be in immediate proximity (effectively merged) at some places, e.g. north of the
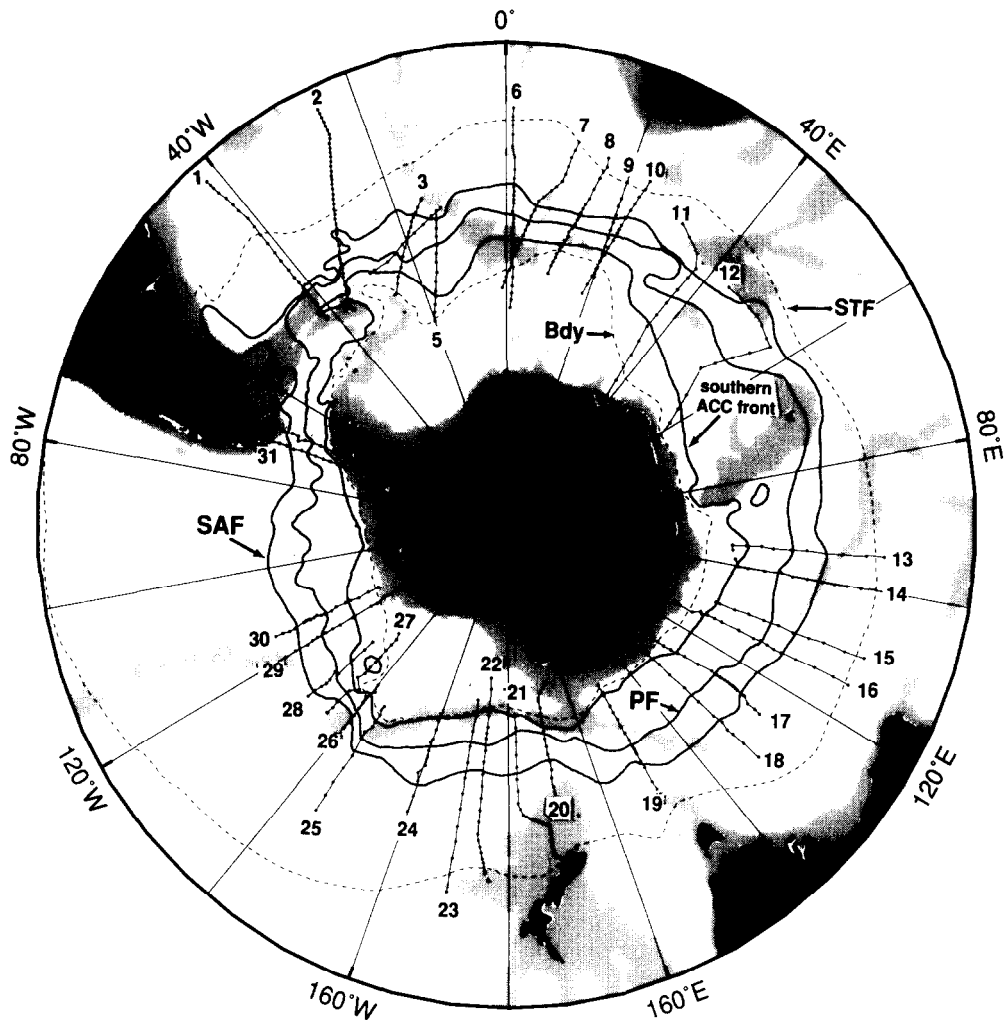
Fig. 11. Circumpolar distributions of the SAF, PF and southern ACC front; the STF and southern boundary of the ACC are also shown as dashed lines. The numbered transects refer to vertical sections listed in Table 4 on which transports and property distributions were examined.

Falkland Plateau (Peterson and Whitworth, 1989; Whitworth *et al.*, 1991), near 32°E (Orsi *et al.*, 1993; Read and Pollard, 1993), north of the Kerguelen Plateau (Park *et al.*, 1993; Belkin and Gordon, 1995), and between the East Pacific Rise and the Pacific–Antarctic Ridge (Patterson and Whitworth, 1990).

Most prominent topographic features influence the path of the southern ACC front. In particular, the Kerguelen Plateau (70°–80°E) clearly obstructs the path of this front and forces it farther to the south. East of the plateau, the southern ACC front turns sharply to the north forming a boundary current along its eastern flank (Speer and Forbes, 1994). In turn, the South Scotia Arc (30°W) deflects this front to the northwest. The southern ACC front also follows very closely the Southwest Indian (5°W–20°E) and the Antarctic–Pacific (160°E–145°W) Ridges. In two particular places the existing data suggest the possible

*Table 4.    Synoptic sections spanning the three ACC fronts*

|     | Ship/cruise | Year | Stations |
|-----|-------------|------|----------|
| 1   | *Melville* SAVE | 1989 | 304–279 |
| 2   | *Melville* SAVE | 1989 | 237–278 |
| 3   | *Islas Orcadas* 16 | 1978 | 218–201 |
| 4   | *Melville* | 1978 | 36–44 |
| 5   | *Islas Orcadas* 16 | 1978 | 219–232 |
| 6   | *Knorr* AJAX | 1984 | 45–49, 64–85 |
| 7   | *Meteor* 11/5 | 1990 | 171–149 |
| 8   | *Islas Orcadas* 11 | 1976 | 56, 51–29 |
| 9   | *Vieze* 716 | 1980 | 21–33 |
| 10  | *Islas Orcadas* 12 | 1977 | 57–75 |
| 11  | *Conrad* 17 | 1974 | 286–179, 252, 278–270 |
| 12  | *Conrad* 17 | 1974 | 220–228, 293–290, 251–238 |
| 13  | *Eltanin* 49 | 1971 | 1364–1373 |
| 14  | *Eltanin* 49 | 1971 | 1386–1374 |
| 15  | *Eltanin* 49 | 1971 | 1346–1356 |
| 16  | *Eltanin* 45,**46** | 1970 | 1267–1253, **2407–2408** |
| 17  | *Eltanin* **39**,37 | 1969 | **1147–1152**, 1099–25, 1096–85 |
| 18  | *Eltanin* 41 | 1970 | 2317–2305 |
| 19  | *Volna* 1348 | 1981 | 18–38 |
| 20  | *Eltanin* 50, **WT-AR2** | 1971 | 1533–1508, **50–52** |
| 21  | *Knorr* KN73 | 1978 | 8–35, 40, 45, 48, 49 |
| 22  | *Knorr* KN73, **GEO** | 1978 | 100–80, 75, 77–79, **287–288** |
| 23  | *Hakuho* M. KH68-4 | 1969 | 35–47 |
| 24  | *Eltanin* 14 | 1964 | 327–344 |
| 25  | *Eltanin* 20 | 1965 | 467–478 |
| 26  | *Eltanin* 19 | 1965 | 455–462 |
| 27  | *Eltanin* 17 | 1965 | 405–416 |
| 28  | *Eltanin* 13 | 1964 | 326–317 |
| 29  | *Eltanin* 33 | 1968 | 829–818 |
| 30  | *Eltanin* 11 | 1964 | 227–245 |
| 31  | *Eltanin* 5 | 1962 | 53–43 |
| 32  | *Eltanin* 5 | 1962 | 28–39 |

generation of eddies from the southern ACC front—indicated by the closed rings in Fig. 11 near 82°E (clockwise) and 135°W (counterclockwise).

Note that over much of its circumpolar extent, the southern ACC front lies close to the boundary (dashed line in Fig. 11) separating the ACC from the subpolar regime. Drake Passage, the Scotia Sea, and the region between 180°W and 140°W are examples. In such areas only very close stations can resolve the two as distinct features.

To summarize, the third, southernmost front in Drake Passage extends continuously around the globe as the southern ACC front. It represents the southernmost current core of the ACC, carrying waters with circumpolar characteristics. This southern front should be included in all estimates of the ACC's property transports. In this study an additional deep front has been recognized between the PF and the southern ACC front in several sections of the ACC, e.g. in the eastern South Indian and Pacific Oceans. However, because its characteristics can not be traced continuously around the globe, no attempt to speculate on its circumpolar nature is made. Reid *et al.* (1995) describe this front at 85°W, and associate it with the "surface" (shallow) expression of the PF at Drake Passage
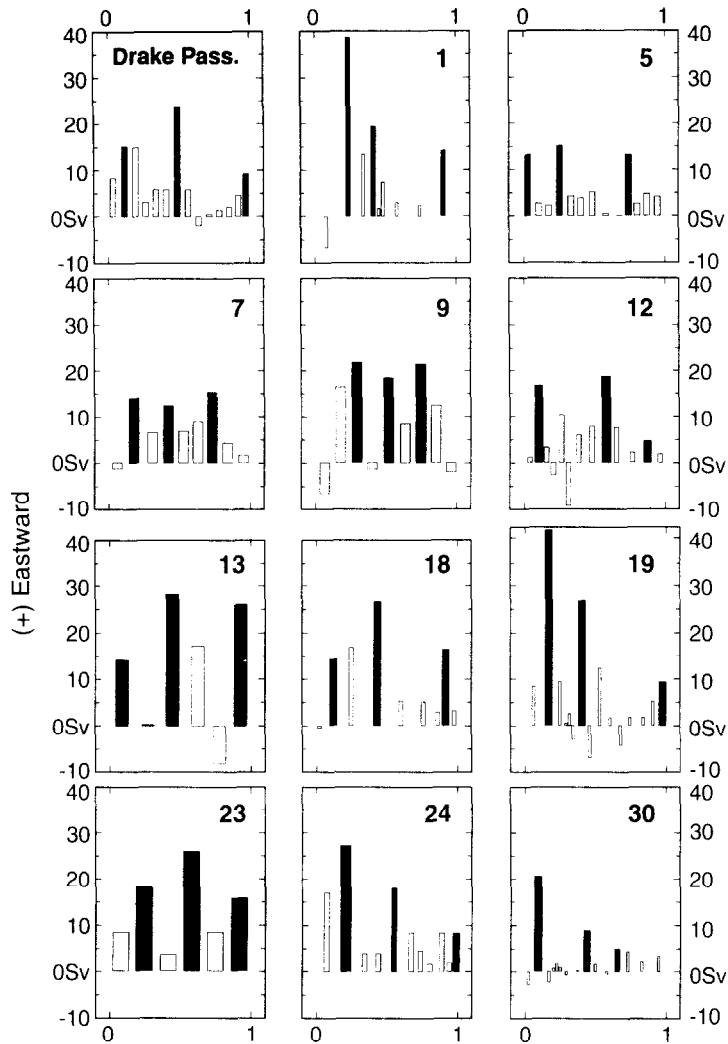
Fig. 12.   Geostrophic volume transport (Sv) relative to 3000 m, or deepest common depth, at
Drake Passage (section 8 in Table 2) and in sections 1, 5, 7, 9, 12, 13, 18, 19, 23, 24 and 30 in Table 4
(Fig. 11); southward alongsection distance is normalized at each section.

reported by Nowlin *et al.* (1977). Nevertheless, it is likely that more details on the fate and characteristics of this and other fronts will result from future densely-sampled sections of the ACC.

### Average stratification of the ACC zones

Some general remarks may be made regarding the water mass structure within the zones separated by the three ACC fronts shown in Fig. 11. Property isolines tend to be nearly horizontal within the ACC zones; most of their depth changes take place at the ACC fronts

(Whitworth and Nowlin, 1987; Sievers and Nowlin, 1984). Using the 32 synoptic sections listed in Table 4, profiles of $\theta$, S and $O_2$ were averaged at standard depths for stations within the same ACC zone to obtain the profiles shown in Fig. 13. Only those stations (94 in number) within a few hundred kilometers of the SAF were considered in the SAZ average. The name "southern" ACC zone in Fig. 13 refers to the region (63 Stas) between the southern ACC front and the southern boundary of the ACC. Average profiles are enclosed by their 95% confidence intervals (dotted envelopes).

Progressive shoaling and weakening toward the south of the characteristic property cores of both the UCDW and LCDW are clear in Fig. 13. Property values for these and other cores of circumpolar water masses are listed in Table 5. In the average, the $O_2$-min of the UCDW rises 1000 m between the SAZ and the southern ACC zone, and increases 0.17 ml $l^{-1}$. Similarly, the S-max of the LCDW rises 1500 m between the same ACC zones, and its salinity decreases 0.03.

In contrast to the CDW, the characteristic signals of waters with Antarctic origin are enhanced toward the south. The "subpolar region" average (Table 5) consists of only 46 Stas located poleward of the southern boundary of the ACC. Waters deeper than 2500 m, i.e. below the S-max, confirm the general cooling and freshening toward the south, as well as enrichment in oxygen concentrations, derived by mixing with denser waters spreading northward from their source regions around Antarctica. This is clearly depicted at the 4000 m level, where from the SAZ to the subpolar region $\theta$ (S) decreases by 1.03°C (0.34), and oxygen increases by 0.66 ml $l^{-1}$.

Temperatures at 100 m decrease southward by about 3°C across both the SAF and PF. Farther to the south, the $\theta$-min of the AASW decreases in temperature by 1.68°C from the AZ to the subpolar region. The SAZ shows an average S-min at 400 m, i.e. above the CDW, which corresponds to the AAIW.

The average property values listed for the subpolar region in Table 5, support the present definition of the southern boundary of the ACC as the poleward bound to the UCDW signal. Both the S-max and $O_2$-min of the subpolar region lie within 100 m of one another (600–700 m), i.e. within the water mass with $\theta$ and S characteristic of LCDW. The average $\theta$-max for this subpolar region lies within LCDW of $\sigma_0 > 27.75$ kg $m^{-3}$ (Sievers and Nowlin, 1984); it is found near 400 m with $\theta = 0.93$°C and S = 34.68. Thus, in contrast to the circumpolar regime, distinct signals of the Upper and Lower CDW can no longer be separated from one another within the subpolar regime.

Property changes of circumpolar waters are evident in the $\theta$-S space. Shown in Fig. 14, the average characteristic curves for the ACC zones are distinct for depths above the S-max of the LCDW. The meridional changes in average properties (Figs 12 and 13) observed across the three ACC fronts confirm the frontal positions presented in Fig. 11. Moreover, since there is no UCDW signal in the subpolar region, as evidenced for instance by the lack of $\theta > 1.5$°C at $\sigma_0 < 27.75$ kg $m^{-3}$, Fig. 14 further validates the position of the poleward boundary of the ACC presented in Fig. 7.

Isopycnal mixing of waters across the ACC fronts may also be inferred from Fig. 14. Surface waters found poleward of the southern ACC front seem to spread northward and contribute to waters near the $\theta$-min of the AZ (75–125 m), approximately along $\sigma_0 = 27.25$ kg $m^{-3}$. A similar process is implied across the PF, approximately along $\sigma_0 = 27.125$ kg $m^{-3}$, as surface waters of the AZ contribute to and influence the subsurface layer of the PFZ (125–175 m). This ACC zone shows the lowest average salinities at 200 m (circled symbols in Fig. 14), in agreement with the observation of Taylor *et al.* (1978) that the PFZ

(a) Potential temperature (C)



(b) Salinity

(c) Oxygen (ml/l)
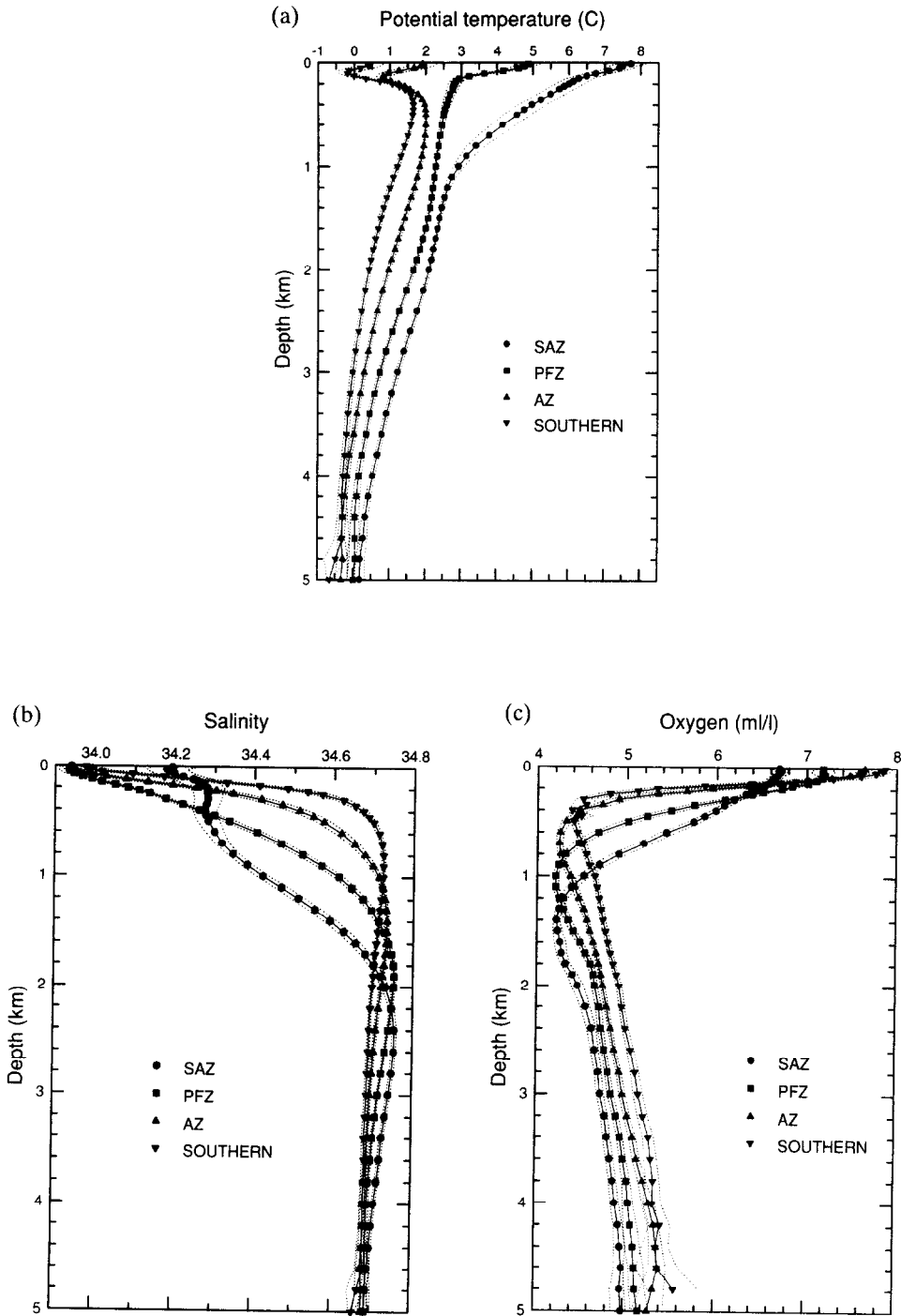


Fig. 13. Average vertical profiles of (a) potential temperature (°C), (b) salinity and (c) dissolved oxygen (ml l$^{-1}$) computed at standard depths for stations shown in Fig. 11. Averages are shown for each zone (number of Stas): SAZ (94), PFZ (111), AZ (113) and southern ACC zone (63); dotted envelopes indicate the 95% confidence intervals.

*Table 5.  Average property values for characteristic cores (maxima and minima) within ACC zones and subpolar region*: Z (m), $\theta$ (°C), S, $O_2$ (ml l$^{-1}$)

|            |         | SAZ      | PFZ      | AZ     | Southern | Subpolar |
|------------|---------|----------|----------|--------|----------|----------|
| $\theta$-min | Z     |          |          | 125    | 100      | 100      |
| (100-m)    | $\theta$ | (6.749)  | (3.635)  | 0.805  | −0.184   | −0.875   |
|            | S       | (34.219) | (33.967) | 34.078 | 34.172   | 34.264   |
|            | $O_2$   | (6.639)  | (7.163)  | 7.021  | 7.290    | 7.264    |
| S-min      | Z       | 400      |          |        |          |          |
|            | S       | 34.275   |          |        |          |          |
|            | $\theta$ | 4.968   |          |        |          |          |
|            | $O_2$   | 5.989    |          |        |          |          |
| $\theta$-max | Z     |          |          | 600    | 400      | 400      |
|            | $\theta$ |          |          | 1.998  | 1.653    | 0.926    |
|            | S       |          |          | 34.619 | 34.673   | 34.676   |
|            | $O_2$   |          |          | 4.256  | 4.386    | 4.750    |
| $O_2$-min  | Z       | 1400     | 1000     | 700    | 400      | 600      |
|            | $O_2$   | 4.217    | 4.216    | 4.245  | 4.386    | 4.706    |
|            | $\theta$ | 2.455   | 2.250    | 1.976  | 1.653    | 0.870    |
|            | S       | 34.592   | 34.620   | 34.652 | 34.673   | 34.698   |
| S-max      | Z       | 2400     | 1900     | 1400   | 900      | 700      |
|            | S       | 34.754   | 34.746   | 34.734 | 34.724   | 34.699   |
|            | $\theta$ | 1.770   | 1.579    | 1.485  | 1.302    | 0.785    |
|            | $O_2$   | 4.618    | 4.661    | 4.558  | 4.585    | 4.729    |
| 4000-m     | $\theta$ | 0.532   | −0.006   | −0.215 | −0.290   | −0.499   |
|            | S       | 34.708   | 34.688   | 34.680 | 34.680   | 34.664   |
|            | $O_2$   | 4.897    | 5.157    | 5.287  | 5.319    | 5.559    |

appears as a band of minimum values on horizontal maps of salinity at that level (see, e.g., Gordon and Molinelli, 1982).

The temperature at the $\theta$-min layer (Fig. 14) decreases southward from the Polar Front, influenced by Winter and Shelf Waters of the subpolar regime. In addition, the salinity of this $\theta$-min lying at the base of the AASW increases progressively southward in Fig. 14 (see also Table 5). This is attributed to the poleward shoaling of relatively saltier UCDW, which eventually enters the mixed layer of the subpolar region.

## CIRCUMPOLAR TRANSPORT

It has been shown that there are three distinct, circumpolar fronts within the ACC. These fronts dominate the total ACC transport at Drake Passage (Nowlin and Clifford, 1982) and at the Greenwich Meridian (Whitworth and Nowlin, 1987). Nevertheless the shear transport carried by each of the ACC fronts varies considerably around the globe, as evidenced by selected sections shown in Fig. 12.

Natural continental boundaries to the ACC simplify the computation of its total geostrophic volume transport at Drake Passage. Even so, early estimates of the baroclinic transport of the ACC at Drake Passage yielded a wide range of values, principally due to selection of different referencing schemes (see Table 1 of Peterson, 1989). Reid and
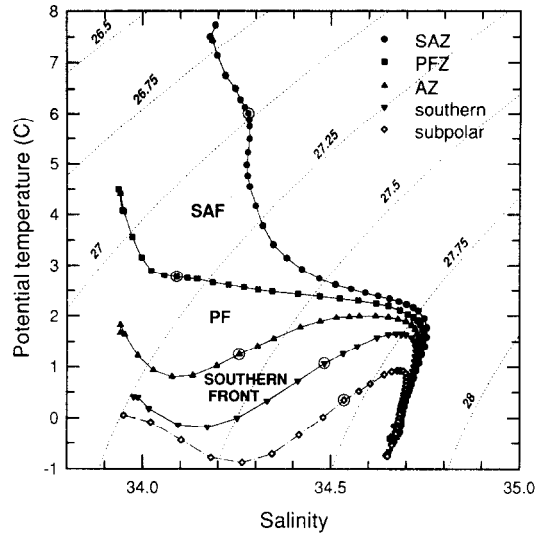
Fig. 14. Potential temperature (°C) versus salinity diagram computed at standard depths for stas shown in Fig. 11. Averages are shown as in Fig. 13, with the addition of the subpolar region based on 46 Stas. Circled symbols indicate the 200 m averages; dotted lines are potential density anomaly $\sigma_0$ (kg m$^{-3}$) isopycnals.

Nowlin (1971) found that for most sections with end stations located sufficiently near the continental margins, whatever its internal distribution, the general pressure field across Drake Passage was remarkably constant. The 13 transects listed in our Table 2 yield an average 97 Sv eastward volume transport through Drake Passage above and relative to 3000 m, with a standard deviation of 13 Sv.

Determination of the ACC transport at locations other than Drake Passage may be biased by the subjective selection of end stations. Underestimates of its total transport may result from the use of hydrographic sections that do not span all three fronts of the ACC. In contrast, overestimates may result if the equatorward or poleward boundaries of the ACC are crossed, thus including part of a subtropical or a subpolar gyre.

Our definition of the southern boundary of the ACC provides a reasonable starting point for the northward integrating transport. Using all the available hydrographic data south of 30°S (Fig. 2), we calculated the geostrophic transport function (Pedlosky, 1987; McLellan, 1965) to portray the approximate volume transport within the ACC. We know from the ISOS that a deep level is a valid reference for the shear transport of the ACC, so the computation was made relative to 3000 m.

The geostrophic transport function

$$T_g = \frac{1}{f} \int_{3000}^{50} \Delta\Phi \, dz,$$

where $f$ is the Coriolis parameter (s$^{-1}$) at a mean latitude and $\Delta\Phi$ is geopotential anomaly (m$^2$ s$^{-2}$), is shown in Fig. 15. The zero-transport contour was placed at the southern side of Drake Passage by subtracting the average transport value there to all other values on the figure.

A fixed latitude of 50°S (roughly in the middle of the ACC band) was used for the
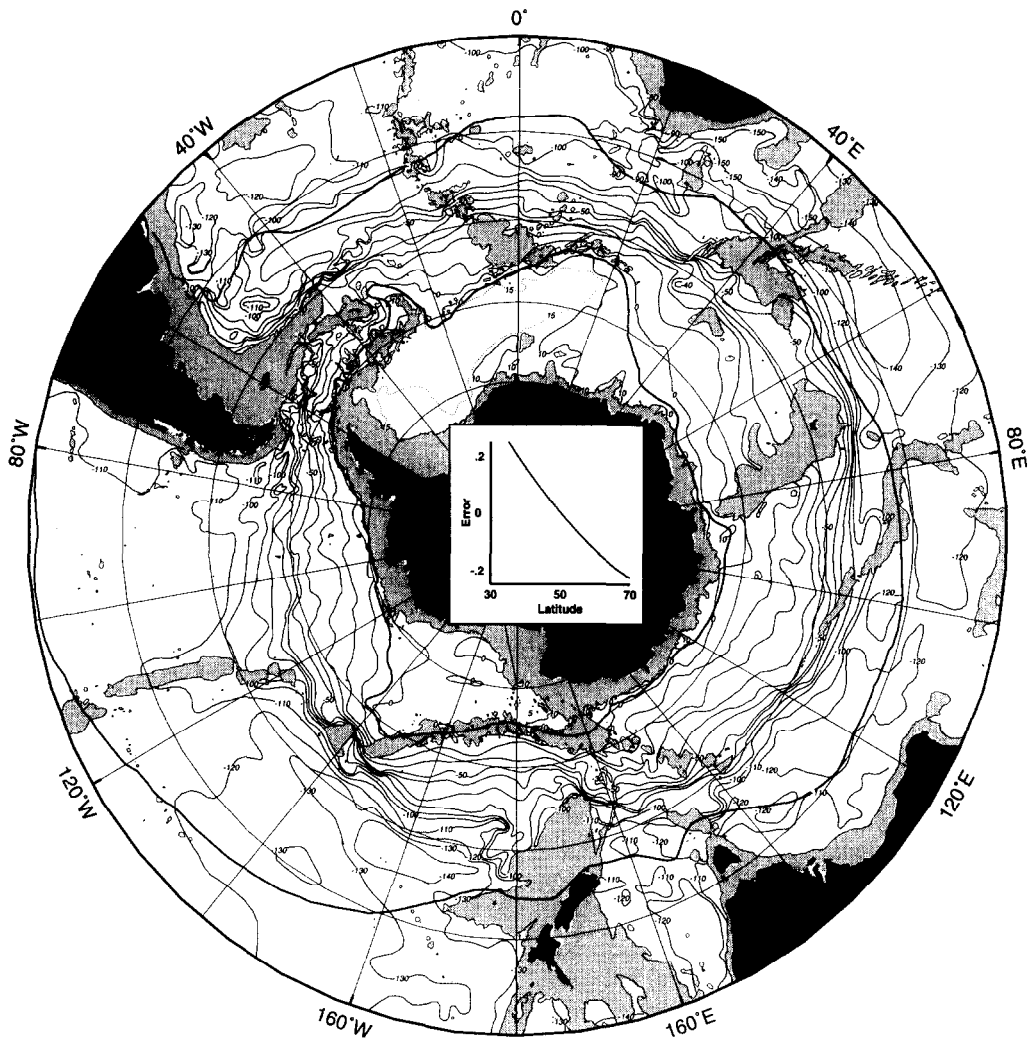
Fig. 15. Geostrophic transport function for the entire Southern Ocean, with 10 Sv contour interval ($1Sv = 10^6 \, m^3 \, s^{-1}$); 50°S is used as the mean latitude to depict the circumpolar flow regime. The graph over Antarctica (inset) shows the fractional error in transport values; heavy lines indicate the location of the STF and the southern boundary of the ACC.

Coriolis parameter. Thus the transport contours in Fig. 15 contain a predictable error, which is generally less than 20% within the meridional bounds of the ACC. The inset shows the fractional error in the transport between two given stations that results from replacing the average latitude of the station pair by 50°S; transport is overestimated south of 50°S and underestimated north of 50°S. Nevertheless, between latitudes of 40°S and 60.75°S the errors compensate almost exactly.

The zero-transport contour was chosen to correspond to the southern ACC boundary at Drake Passage, but Fig. 15 shows that elsewhere there is good agreement between the contour and the poleward edge of the ACC. The transport through Drake Passage is about

100 Sv, in excellent agreement with the mean transport (97 Sv) computed conventionally for the sections in Table 2. The 100-Sv contour is nearly everywhere south of the STF (Fig. 15) and north of the SAF (Fig. 11), indicating an ACC transport of about 100 Sv relative to 3000 m. As Gill and Bryan (1971) pointed out, the absence of topographic barriers in a zonal band means that there can be no pressure difference to balance the Coriolis force per unit area, and thus no net meridional flow across such a band. Inflows to the ACC must then roughly balance outflow into neighboring regimes within the 50–3000 m layer, and 100 Sv is a conservative estimate of the ACC transport in open-ocean locations.

South of the 0-Sv contour in Fig. 15, the Weddell Gyre appears as the largest cyclonic circulation of the subpolar regime. It carries about 15 Sv of shear flow above 3000 m, whereas the rest of the subpolar regime carries no more than 10 Sv. A relatively weak cyclonic flow (<10 Sv) is implied in the Ross Gyre. Note that near the Antarctic continental margins, selection of a shallower reference level could also render westward flow over many near-shelf areas.

## SUMMARY

Hydrographic observations were used in this study of the Southern Ocean to improve our knowledge of large-scale aspects of the Antarctic Circumpolar Current. The flow associated with this current appears in the dynamic topography of the upper kilometer of water (50/1000 db), as a zonal band with continuous contours through Drake Passage. This ACC band shows relatively large geostrophic shear, when compared with the adjacent circulations in the subtropical and subpolar regimes. However, the flow is similarly sheared in the southern limbs of the subtropical gyres, particularly near the western boundary of each ocean basin, making differentiation of the ACC and subtropical regimes difficult based on shear alone.

The Subtropical Front is considered the northern limit of the Subantarctic Surface Waters. Following Deacon's original definition of the Subtropical Convergence, the STF is delineated by means of property maps at a near-surface level (100 m). There is a narrow transition between warm and saline surface waters of the subtropical regime and colder and fresher subantarctic waters. Although many stations have been added since Deacon (1982) prepared his maps, this band is found to closely follow his position of the Subtropical Convergence (now referred to as Front).

Closely-spaced stations along the Greenwich Meridian reveal a sharp termination to the poleward extent of Upper Circumpolar Deep Water characteristics, which coincides with a frontal feature that separates the ACC from the Weddell Gyre. Property maps on a density surface characterizing the UCDW core within the ACC show a clear transitional band around Antarctica, across which the selected isopycnal shoals to within 200 m of the surface. South of this band, the characteristic signal of the UCDW is no longer discernible; most of this water mass has been entrained into the surface mixed layer and its identifying isopycnal lies within Antarctic Surface Water. Examination of numerous transects through this transition allowed us to trace the southern limit of UCDW characteristics. Its location is in good agreement with the observed change in geostrophic shear between the ACC and the subpolar circulations. This water mass boundary is suggested as a useful definition of the southern boundary of the ACC.

Recent high-quality transects of the ACC at Drake Passage average 97 Sv of eastward baroclinic transport above 3000 m. In the open ocean far from Drake Passage, more

consistent estimates of the current's baroclinic transport result naturally from the present definition of its southern boundary. A geostrophic transport function map for the Southern Ocean reveals that roughly 100 Sv are transported to the east above 3000 m at all longitudes within the proposed meridional boundaries of the circumpolar regime.

The characteristic frontal structure between the meridional bounds of the ACC was examined. Previous observations have shown three deep-reaching fronts at both the Drake Passage and Greenwich Meridian. These ACC fronts appear as maxima in geostrophic transport and show distinct property characteristics at both locations. Examination of water mass properties (tracers) and volume transport estimates reveal three fronts on all synoptic sections across the ACC. The name southern ACC front is proposed here for the third, southernmost of these circumpolar current cores.

Based on examination of property changes and zonal shear transports from all meridional sections, presented here, for the first time, are circumpolar paths for the SAF, PF and the southern ACC front. As portrayed by zonally-averaged $\theta$–S relations for waters above Lower Circumpolar Deep Water, the fronts separate distinctly different water mass regimes. Zonally-averaged characteristic curves also show the northward spread and mixing along isopycnals of surface waters across the southern ACC front, which contribute to the subsurface temperature minimum layer of the Antarctic Zone. A similar influence is also implied across the Polar Front.

In the average, the characteristic temperature minimum of the Antarctic Surface Water becomes saltier and colder to the south of the Polar Front. It is the saltiest in the subpolar region, suggesting the progressive entrainment of UCDW from the ACC into the mixed layer of the subpolar regime.

This identification of the major large-scale features of the ACC is expected to benefit future descriptive studies and numerical simulations. In particular, all three deep-reaching fronts of the ACC should be included in quantitative analyses and models of this current. The present delineation of its southern end may aid also in estimating and understanding property exchanges between the ACC and the subpolar regime.

## REFERENCES

Bagriantsev N. V., A. L. Gordon and B. A. Huber (1989) Weddell Gyre: temperature maximum stratum. *Journal of Geophysical Research*, **94**, 8331–8334.

Belkin I. M. and A. L. Gordon (1995) Southern Ocean fronts from the Greenwich Meridian to Tasmania. Submitted to *Journal of Geophysical Research*.

Callahan J. E. (1972) The structure and circulation of deep water in the Antarctic. *Deep-Sea Research*, **19**, 563–575.

Carmack E. C. and P. D. Killworth (1978) Formation and interleaving of abyssal water masses off Wilkes Land, Antarctica. *Deep-Sea Resarch*, **25**, 357–370.

Clifford M. A. (1983) A descriptive study of the zonation of the Antarctic Circumpolar Current and its relation to wind stress and ice cover. Unpublished MS thesis, Texas A&M University, 93 pp.

Deacon G. E. R. (1933) A general account of the hydrology of the South Atlantic Ocean. *Discovery Reports*, **7**, 171–238.

Deacon G. E. R. (1937) The hydrology of the Southern Ocean. *Discovery Reports*, **15**, 1–24.

Deacon G. E. R. (1977) Comments on a counterclockwise circulation in the Pacific subantarctic sector of the Southern Ocean suggested by McGinnis. *Deep-Sea Research*, **24**, 927–930.

Deacon G. E. R. (1979) The Weddell Gyre. *Deep-Sea Research*, **26**, 981–995.

Deacon G. E. R. (1982) Physical and biological zonation in the Southern Ocean. *Deep-Sea Research*, **29**, 1–15.

Emery W. J. (1977) Antarctic Polar Frontal Zone from Australia to the Drake Passage. *Journal of Physical Oceanography*, **7**, 811–822.

Foster T. D. and E. C. Carmack (1976) Frontal zone mixing and Antarctic Bottom Water formation in the southern Weddell Sea. *Deep-Sea Research*, **23**, 301–317.

Gill A. E. (1973) Circulation and bottom water production in the Weddell Sea. *Deep-Sea Research*, **20**, 111–140.

Gill A. E. and K. Bryan (1971) Effects of geometry on the circulation of a three-dimensional southern-hemisphere ocean model. *Deep-Sea Research*, **18**, 685–721.

Gordon A. L. (1967) Structure of Antarctic waters between 20°W and 170°W. In: *Antarctic map folio series*, Folio 6, V. C. Bushnell, editor, American Geography Society, 10 pp.

Gordon A. L. (1971) Antarctic Polar Front Zone. In: *Antarctic oceanology I, antarctic research series*, 15, J. L. Reid, editor, American Geophysical Union, Washington, DC., 205–221.

Gordon A. L. (1974) Varieties and variability of Antarctic Bottom Water. *Colloques internationals du Centre national de la recherche scientifique*, **215**, Processus de formation des eaux oceaniques profondes, 33–47.

Gordon A. L. (1988) Spatial and temporal variability within the Southern Ocean. In: *Antarctic ocean and resources variability*, D. Sahrhage, editor, Springer–Verlag, Berlin, 41–56.

Gordon A. L. and P. T. Tchernia (1972) Waters of the continental margin off Adelie Coast, Antarctica. In: *Antarctic oceanography II: the Australian-New Zealand sector*, Antarctic Research Series, Vol. 9, D. E. Hayes, editor, American Geophysical Union, pp. 59–69.

Gordon A. L. and E. Molinelli (1982) *Southern ocean atlas*. Columbia University Press, New York, 11 pp., 233 plates.

Gordon A. L., H. W. Taylor and D. T. Georgi (1977a) Antarctic oceanographic zonation. In: *Proceedings of the SCOR/SCAR polar oceans conference, May 5–11, 1974*. International Oceanographic Commission, McGill University, Montreal, pp. 45–76.

Gordon A. L., D. T. Georgi and H. W. Taylor (1977b) Antarctic Polar Front zone in the western Scotia Sea-Summer 1975. *Journal of Physical Oceanography*, **7**, 309–328.

Gordon A. L., E. Molinelli and T. Baker (1978) Large-scale relative dynamic topography of the Southern Ocean. *Journal of Geophysical Research*, **83**, 3023–3032.

Heath R. A. (1981) Oceanic fronts around southern New Zealand. *Deep-Sea Research*, **28**, 547–560.

Hofmann E. E. (1985) The large-scale horizontal structure of the Antarctic Circumpolar Current from FGGE drifters. *Journal of Geophysical Research*, **90**, 7087–7097.

Hofmann E. E., B. L. Lipphardt Jr, R. A. Locarnini and D. A. Smith (1993) Palmer LTER: hydrography in the LTER region. *Antarctic Journal of the United States*, **XXVIII**, 5, 209–211.

Jacobs S. S., A. F. Amos and P. M. Bruchhausen (1970) Ross Sea oceanography and antarctic bottom water formation. *Deep-Sea Research*, **17**, 935–962.

Jacobs S. S. and D. T. Georgi (1977) Observations on the southwest Indian/Antarctic Ocean. In: *Voyage of discovery*, M. Angel, editor, Oergamon, New York, pp. 43–85.

Locarnini R. A. (1994) Water masses and circulation in the Ross Gyre and environs. Unpublished MS thesis, Texas A and M University, College Station, 87 pp.

McLellan H. J. (1965) *Elements of physical oceanography*. Pergamon Press, London, 151 pp.

Mantyla A. W. and J. L. Reid (1983) Abyssal characteristics of the Worlds Ocean waters. *Deep-Sea Research*, **30**, 805–833.

Neshyba S. and T. R. Fonseca (1980) Evidence for counterflow to the West Wind Drift off South America. *Journal of Geophysical Research*, **85**, 4888–4892.

Nowlin W. D. Jr and M. Clifford (1982) The kinematic and thermohaline zonation of the Antarctic Circumpolar Current at Drake Passage. *Journal of Marine Research*, **40**, 481–507.

Nowlin W. D. Jr and W. Zenk (1988) Westward currents along the margin of the South Shetland Island Arc. *Deep-Sea Research*, **35**, 269–301.

Nowlin W. D. Jr, T. Whitworth III and R. D. Pillsbury (1977) Structure and transport of the Antarctic Circumpolar Current at Drake Passage from short-term measurements. *Journal of Physical Oceanography*, **7**, 778–802.

Orsi A. H., W. D. Nowlin Jr and T. Whitworth III (1993) On the circulation and stratification of the Weddell Gyre. *Deep-Sea Research I*, **40**, 169–203.

Park Y. H., L. Gamberoni and E. Charriaud (1993) Frontal structure, water masses, and circulation in the Crozet Basin. *Journal of Geophysical Research*, **98**, 12361–12385.

Patterson S. L. and T. Whitworth III (1990) Physical oceanography of the Pacific sector of the Southern Ocean. In: *Antarctic sector of the Pacific*, G. P. Glasby, editor, Elsevier Oceanography Series, Vol. 51, Amsterdam, pp. 55–93.

Pedlosky J. (1987) Geophysical Fluid Dynamics, 2nd edition. Springer–Verlag, New York, 710 pp.

Peterson R. G. (1989) On the variability of the Antarctic Circumpolar Current. Unpublished PhD thesis, Texas A&M University, 97 pp.

Peterson R. G. and T. Whitworth III (1989) The Subantarctic and Polar Fronts in relation to deep water masses through the southwestern Atlantic. *Journal of Geophysical Research*, **94**, 10817–10838.

Peterson R. G. and L. Stramma (1991) Upper-level circulation in the South Atlantic Ocean. *Progress in Oceanography*, **26**, 1–73.

Pickard G. L. (1971) Some physical oceanographic features of inlets of Chile. *Journal of Fisheries Research Board of Canada*, **28**, 1077–1106.

Potter J. R. and J. G. Paren (1984) Interaction between ice shelf and ocean in George VI Sound, Antarctica. In: *Oceanology of the Antarctica Continental Shelf* S. S. Jacobs, editor, Antarctic Research Series, Vol 43, pp. 35–58.

Read J. F. and R. T. Pollard (1993) Structure and transport of the Antarctic Circumpolar Current and Agulhas Return Current at 40°E. *Journal of Geophysical Research*, **98**, 12281–12295.

Read J. F., R. T. Pollard, A. I. Morrison and C. Symon (1995) On the southerly extent of the Antarctic Circumpolar Current in the southeast Pacific. Submitted to *Journal of Geophysical Research*.

Reid J. L. (1965) Intermediate waters of the Pacific Ocean. *Johns Hopkins Oceanographic Studies*, **2**, 85 pp.

Reid J. L. (1986) On the total geostrophic circulation of the South Pacific Ocean: Flow patterns, tracers and transports. *Progress in Oceanography*, **16**, 1–61.

Reid J. L. (1989) On the total geostrophic circulation of the South Atlantic Ocean: Flow patterns, tracers and transports. *Progress in Oceanography*, **23**, 149–244.

Reid J. L. and R. J. Lynn (1971) On the influence of the Norwegian–Greenland and Weddell seas upon the bottom waters of the Indian and Pacific oceans. *Deep-Sea Research*, **18**, 1063–1088.

Reid J. L. and A. W. Mantyla (1971) Antarctic work of the Aries expedition. *Antarctic Journal of the United States*, **4**, 111–113.

Reid J. L. and W. D. Nowlin Jr (1971) Transport of water through the Drake Passage. *Deep-Sea Research*, **18**, 51–64.

Reid J. L., W. D. Nowlin Jr and W. C. Patzert (1977) On the characteristics and circulation of the southwestern Atlantic Ocean. *Journal of Physical Oceanography*, **7**, 62–91.

Rodman M. R. and A. L. Gordon (1982) Southern Ocean bottom water of the Australian–New Zealand sector. *Journal of Geophysical Research*, **87**, 5771–5778.

Roether W., R. Schlitzer, A. Putzka, P. Beining, K. Bulsiewicz, G. Rohardt and F. Delahoyde (1993) A chlorofluoromethane and hydrographic section across Drake Passage: deep water ventilation and meridional property transport. *Journal of Geophysical Research*, **98**, 14423–14435.

Sievers H. A. and W. J. Emery (1978) Variability of the Antarctic Polar Frontal Zone in Drake Passage— Summer 1976–1977. *Journal of Geophysical Research*, **83**, 3010–3022.

Sievers H. A. and W. D. Nowlin Jr (1984) The stratification and water masses at Drake Passage. *Journal of Geophysical Research*, **89**, 10489–10514.

Sievers H. A. and W. D. Nowlin Jr (1988) Upper ocean characteristics in Drake Passage and adjoining areas of the Southern Ocean, 39°W–95°W. In: *Antarctic and resources variability*, D. Sahrhage, editor, Springer– Verlag, Berlin, pp. 57–80.

Silva Sandoval N. R. (1977) Water mass structure and circulation off southern Chile. MS Thesis, School of Oceanography, Oregon State University, Corvalis, 1–83.

Smith S. G. (1989) On the Weddell-Scotia Confluence and the Scotia Front. Unpublished MS thesis, Texas A&M University, College Station, 101 pp.

Speer K. G. and A. Forbes (1994) A deep western boundary current in the South Indian Basin. *Deep-Sea Research*, **41**, 1289–1303.

Stramma L. (1992) The South Indian Ocean Current. *Journal of Physical Oceanography*, **22**, 421–430.

Stramma L. and R. G. Peterson (1990) The South Atlantic Current. *Journal of Physical Oceanography*, **20**, 846– 859.

Stramma L., R. G. Peterson and M. Tomczak (1995) The South Pacific Current. *Journal of Physical Oceanography*, **25**, 77–91.

Talbot M. H. (1988) Oceanic environment of George VI ice shelf, Antarctica Peninsula. *Annals of Glaciology*, **11**, 161–164.

Taylor H. W., A. L. Gordon and E. Molinelli (1978) Climatic characteristics of the Antarctic Polar Zone. *Journal of Geophysical Research*, **83**, 4572–4578.

Tchernia P. and P. F. Jeannin (1983) *Quelques aspects de la circulation oceanique Antarctique reveles par l'observation de la derive d'icebergs* (1972–1983). Centre Nat d'Etudes Spatiales. Mus Nat Hist Nat, Paris, 92 pp.

Trenberth K. E., W. G. Large and J. G. Olson (1990) The mean annual cycle in global ocean wind stress. *Journal of Physical Oceanography*, **30**, 1742–1760.

Treshnikov A. F., A. A. Girs, G. I. Baranov and V. A. Yefimov (1973) Preliminary programme of the Polar Experiment for the South Polar Region, Arctic and Antarctic Research Institute, Leningrad, U.S.S.R., 55 pp.

Warren B. A. (1981) Transindian hydrographic section at Lat. 18°S: property distributions and circulation in the South Indian Ocean. *Deep-Sea Research*, **28**, 759–788.

Whitworth T. III (1980) Zonation and geostrophic flow of the Antarctic Circumpolar Current at Drake Passage. *Deep-Sea Research*, **27**, 497–507.

Whitworth T. III and W. D. Nowlin Jr (1987) Water masses and currents of the southern ocean at the Greenwich Meridian. *Journal of Geophysical Research*, **92**, 6462–6476.

Whitworth T. III, W. D. Nowlin Jr and S. J. Worley (1982) The net transport of the Antarctic Circumpolar Current through Drake Passage. *Journal of Physical Oceanography*, **12**, 960–971.

Whitworth T. III, W. D. Nowlin Jr, R. D. Pillsbury, M. I. Moore and R. F. Weiss (1991) Observations of the Antarctic Circumpolar Current and deep western boundary current in the southwestern Atlantic. *Journal of Geophysical Research*, **96**, 15105–15118.